

First Paramagnetic Zerovalent Transition Metal Isocyanides. Syntheses, Structural Characterizations, and Magnetic Properties of Novel Low-Valent Isocyanide Complexes of Vanadium¹

Mikhail V. Barybin,^{*,†} Victor G. Young, Jr., and John E. Ellis^{*}

Contribution from the Department of Chemistry, University of Minnesota, Minneapolis, Minnesota 55455

Received January 20, 2000

Abstract: The first homoleptic paramagnetic transition metal isocyanide, V(CNXyl)₆ (**2**, Xyl = 2,6-dimethylphenyl), can be isolated in high yield by reacting bis(naphthalene)vanadium(0) (**1a**) or bis(1-methylnaphthalene)vanadium(0) (**1b**) with 6 equiv of CNXyl in tetrahydrofuran/heptane. Reduction of **2** with excess cesium graphite in THF affords excellent yields of [V(CNXyl)₆][−] (**3**) as an unsolvated Cs⁺ salt, the first homoleptic octahedral isocyanide metalate. Cs**3** reacts with 2 equiv of 18-Crown-6 to give [Cs(18-Crown-6)₂]**3**. Anion **3** can also be isolated as a practically insoluble [K(Crypt{2.2.2.})]⁺ salt by reducing **2** with potassium naphthalenide in the presence of Crypt{2.2.2.}. Complex **3** reduces [Et₃NH]Cl to form paramagnetic **2**. Oxidation of **2** by ferricinium hexafluorophosphate in THF provides nearly quantitative yields of the 16-electron paramagnetic [V(CNXyl)₆][PF₆][−] (**4**[PF₆]), analogous to the exceedingly unstable [V(CO)₆]⁺. Interaction of V(CO)₆ with excess CNXyl in heptane results in the efficient formation of *trans*-[V(CO)₂(CNXyl)₄] (**5**). Such a substitution reaction is highly unusual for V(CO)₆. Oxidation of compound **5** by ferricinium hexafluorophosphate in THF affords homoleptic **4**[PF₆]. Complexes **2**, **3**, **4**, and **5** were characterized by a variety of spectroscopic methods and X-ray crystallography. Spectroscopic, magnetic, and structural features of these novel electron rich vanadium isocyanides are discussed in detail. The average V–CN bond length increases in the series [V(CNXyl)₆][−] < V(CNXyl)₆ < *trans*-V(CO)₂(CNXyl)₄ < [V(CNXyl)₆]⁺. Well-resolved ¹H and ¹³C NMR spectra were obtained for paramagnetic **2** and its chromium congener, [Cr(CNXyl)₆]⁺. The importance of back-bonding in the mechanism of unpaired spin delocalization within **2** was demonstrated. Contrary to the previous prediction for dπ(M)–pπ*(L) unpaired spin delocalization in low-spin d⁵ octahedral complexes, negative spin appears to be induced on the CNXyl ligands of **2** by means of dπ(V)–pπ*(CNXyl) back-bonding.

Introduction

Similar to metal carbonyls, complexes of transition metals with isocyanides have been proven to be valuable reagents in synthetic chemistry and catalysis.² One of the first recognized substantial differences between carbon monoxide and isocyanides as ligands was the fact that the former seemed to be ideal for stabilizing zero- and subvalent metals while the latter were most common in complexes of metals with higher oxidation states. As it was pointed out in 1998, “the number of neutral homoleptic metal carbonyls known clearly exceeds that of the corresponding isocyanide complexes”.^{2g} The lack of zerovalent isocyanides of the elements with odd atomic numbers and isocyanide analogues of carbonyl metalates was originally emphasized in 1959.^{2a} Only 18 years later the first zerovalent isocyanides of an “odd” metal, Co₂(CNR)₈ (R = ^tBu, Xyl, 4-Br-Xyl, Mes), were prepared.³ These neutral compounds are

diamagnetic and have dimeric structures^{4,5} with a Co–Co bond supported by two bridging CNR ligands in the solid state, similar to their carbonyl congener Co₂(CO)₈.⁶ Until the work presented herein, no mononuclear (and, hence, paramagnetic) complexes of this class were known. The elegant study by Cooper and Warnock, describing isolation of the initial homoleptic isocyanide metalate, [Co(CNXyl)₄][−], appeared in 1989.^{5,7}

Despite the original claim that group 5 transition metals “did not show any tendency to form complexes with isocyanides”,^{2a} a number of such species have been subsequently reported. These include Lippard’s [V(CN^tBu)₆]²⁺,⁸ which remained the sole homoleptic group 5 metal isocyanide prior to our recent contributions.⁹ Most vanadium isocyanides, isolated to date, contain the metal in a positive formal oxidation state.¹⁰ In these

[†] Present address: Department of Chemistry, MIT, Cambridge, MA 02139.

(1) Highly Reduced Organometallics. Part 53. Part 52: Chen, Y. S.; Ellis, J. E. *Inorg. Chim. Acta*. In press.

(2) For reviews on transition metal complexes with isocyanides see: (a) Malatesta, L. *Progr. Inorg. Chem.* **1959**, *1*, 283. (b) Malatesta, L.; Bonati, F. *Isocyanide Complexes of Transition Metals*; Wiley: New York, 1969. (c) Treichel, P. M. *Adv. Organomet. Chem.* **1973**, *11*, 21. (d) Bonati, F.; Minghetti, G. *Inorg. Chim. Acta* **1974**, *9*, 95. (e) Yamamoto, Y. *Coord. Chem. Rev.* **1980**, *32*, 193. (f) Singleton, E.; Oosthuizen, H. E. *Adv. Organomet. Chem.* **1983**, *22*, 209. (g) Weber, L. *Angew. Chem., Int. Ed.* **1998**, *37*, 1515.

(3) (a) Barker, G. K.; Galas, A. M. R.; Green, M.; Howard, J. A. K.; Stone, F. G. A.; Turney, T. W.; Welch, A. J.; Woodward, P. J. *Chem. Soc., Chem. Commun.* **1977**, 256. (b) Yamamoto, Y.; Yamazaki, H. *Inorg. Chem.* **1978**, *17*, 3111.

(4) Carroll, W. E.; Green, M.; Galas, A. M. R.; Murray, M.; Turney, T. W.; Welch, A. J.; Woodward, P. J. *Chem. Soc., Dalton Trans.* **1980**, 80.

(5) Leach, P. A.; Geib, S. J.; Corella, J. A., II; Warnock, G. F.; Cooper, N. J. *J. Am. Chem. Soc.* **1994**, *116*, 8566.

(6) Sumner, G. G.; Klug, H. P.; Alexander, L. E. *Acta Crystallogr.* **1964**, *17*, 732.

(7) Warnock, G. F.; Cooper, N. J. *Organometallics* **1989**, *8*, 1826. See also ref 5.

(8) (a) Silverman, L. D.; Dewan, J. C.; Giandomenico, C. M.; Lippard, S. J. *Inorg. Chem.* **1980**, *19*, 3379. (b) Silverman, L. D.; Corfield, P. W. R.; Lippard, S. J. *Inorg. Chem.* **1981**, *20*, 3106.

complexes the CNR ligands function primarily as σ -donors.^{2g,10e} Given the diversity of group 6 metal(0) isocyanides,^{2e} the lack of any V(0) compounds possessing at least one isocyanide ligand is striking. It is worth mentioning that cyclic voltammograms of $[\text{V}(\text{CN}^t\text{Bu})_6]^{2+}$ revealed one reversible ($E_{1/2} = -0.95$ V) and one quasireversible ($E_{1/2} \approx -1.5$ V) wave assigned to $[\text{V}(\text{CN}^t\text{Bu})_6]^{2+/+}$ and $[\text{V}(\text{CN}^t\text{Bu})_6]^{+/0}$ couples, respectively.¹¹ No other data on the otherwise elusive species $[\text{V}(\text{CN}^t\text{Bu})_6]^{+/0}$ are available. Complexes *cis*- $[\text{V}(\text{NO})_2(\text{CNR})_4]^+$,^{12a} $\text{CpV}(\text{NO})_2(\text{CNR})$,^{12b} $\text{VX}(\text{NO})_2(\text{CNR})_3$,^{12c} and $[\text{V}(\text{CO})_5(\text{CNR})]^-$ ¹³ represent the only examples of subvalent vanadium isocyanides. On the basis of usual conventions,² the above nitrosyl–isocyanide compounds are formally classified as derivatives of V(1–). However, as evidenced by IR data in the ν_{CN} region, the CNR ligands in these complexes are not much different electronically from those in the V(2+) compounds. Indeed, the C–N stretching bands of, for example, $[\text{V}(\text{NO})_2(\text{CN}^t\text{Bu})_4]^+$ occur at 2199 and 2183 cm^{-1} ,^{12a} while $[\text{V}(\text{CN}^t\text{Bu})_6]^{2+}$ absorbs at 2190 cm^{-1} .^{8a}

The well-established propensity of group 5 transition metals to induce reductive coupling and polymerization of isocyanides^{10a,14} together with the fact that a highly reduced metal center should facilitate carbon–carbon bond formation between CNR molecules^{14a} may explain the scarcity of low-valent vanadium isocyanides. In this article, we report on the chemistry of new thermally stable electron rich isocyanide complexes of vanadium. Of particular significance are the first paramagnetic zerovalent metal isocyanides, $\text{V}(\text{CNXyl})_6$ and *trans*- $\text{V}(\text{CO})_2(\text{CNXyl})_4$ (Xyl = 2,6-dimethylphenyl). Remarkably, the former 17-electron homoleptic compound is the only binary octahedral paramagnetic metal(0) complex for which well-resolved NMR spectra have been recorded.¹⁵ Analysis of the ¹H and ¹³C NMR patterns, obtained for $\text{V}(\text{CNXyl})_6$, in terms of unpaired spin delocalization is presented. Also described are the first 16- and 18-electron homoleptic isocyanide complexes of vanadium, namely $[\text{V}(\text{CNXyl})_6]^+$ and $[\text{V}(\text{CNXyl})_6]^-$. The latter ion and its tantalum congener, $[\text{Ta}(\text{CNXyl})_6]^-$,^{9b} constitute the first binary octahedral isocyanide metalates.

(9) (a) Barybin, M. V.; Young, V. G., Jr.; Ellis, J. E. *J. Am. Chem. Soc.* **1998**, *120*, 429. (b) Barybin, M. V.; Young, V. G., Jr.; Ellis, J. E. *J. Am. Chem. Soc.* **1999**, *121*, 9237.

(10) (a) Rehder, D.; Böttcher, C.; Collazo, C.; Hedelt, R.; Schmidt, H. *J. Organomet. Chem.* **1999**, *585*, 294. (b) Böttcher, C.; Schmidt, H.; Rehder, D. *J. Organomet. Chem.* **1999**, *580*, 72. (c) Davies, S. C.; Hughes, D. L.; Janas, Z.; Jerzykiewicz, L.; Richards, R. L.; Sanders, J. R.; Sobota, P. *Chem. Commun.* **1997**, *14*, 1261. (d) Nomura, K.; Schrock, R. R.; Davis, W. M. *Inorg. Chem.* **1996**, *35*, 3695. (e) Böttcher, C.; Rodewald, D.; Rehder, D. *J. Organomet. Chem.* **1995**, *496*, 43. (f) Petillon, F. Y.; Schollhammer, P.; Talarmin, J. *J. Organomet. Chem.* **1991**, *411*, 159. (g) Carafoglio, T.; Floriani, C.; Chiesi-Villa, A.; Guastini, C. *Inorg. Chem.* **1989**, *28*, 4417. (h) Anderson, S. J.; Wells, F. J.; Wilkinson, G.; Hussain, B.; Hursthouse, M. B. *Polyhedron* **1988**, *7*, 2615. (i) Coville, N. J.; Harris, G. W.; Rehder, D. *J. Organomet. Chem.* **1985**, *293*, 365. (j) Fachinetti, G.; Del Nero, S.; Floriani, C. *J. Chem. Soc., Dalton Trans.* **1976**, 1046. (k) Crociani, B.; Nicolini, M.; Richards, R. L. *J. Organomet. Chem.* **1975**, *101*, C1.

(11) Shah, S. S.; Maverick, A. W. *J. Chem. Soc., Dalton Trans.* **1987**, 2881.

(12) (a) Herberhold, M.; Trampisch, H. *Inorg. Chim. Acta* **1983**, *70*, 143. (b) Herberhold, M.; Trampisch, Z. *Naturforsch.* **1982**, *37b*, 614. (c) Nümann, F.; Rehder, D. *Z. Naturforsch.* **1984**, *39b*, 1654.

(13) (a) Ellis, J. E.; Fjare, K. L. *Organometallics* **1982**, *1*, 898. (b) Ihmels, K.; Rehder, D. *Organometallics* **1985**, *4*, 1340.

(14) (a) Carnahan, E. M.; Protasiewicz, J. D.; Lippard, S. J. *Acc. Chem. Res.* **1993**, *26*, 90 and references therein. (b) Collazo, C.; Rodewald, D.; Schmidt, H.; Rehder, D. *Organometallics* **1996**, *15*, 4884 and references therein. (c) Rehder, D.; Gailus, H. *Trends Organomet. Chem.* **1994**, *1*, 397 and references therein.

(15) For instance, an ¹H NMR spectrum of $\text{Co}(\text{PPh}_2\text{Me})_4$, a homoleptic paramagnetic metal(0) complex, has been obtained (La Mar, G. N.; Sherman, E. O.; Fuchs, G. A. *J. Coord. Chem.* **1971**, *1*, 289). The tetrahedral geometry of this molecule has been assumed solely based on the very narrow line width of the ¹H NMR peaks.

Experimental Section

General Procedures, Starting Materials, and Equipment. All operations were performed under an atmosphere of 99.5% argon further purified by passage through columns of activated BASF catalyst and molecular sieves. All connections involving the gas purification systems were made of glass, metal, or other materials impermeable to air. Solutions and slurries were transferred via stainless steel needles (cannulas) whenever possible. Standard Schlenk techniques were employed with a double manifold vacuum line.¹⁶ Solvents were freed of impurities by standard procedures and stored under argon. Naphthalene was sublimed under vacuum and 1-methylnaphthalene was distilled under reduced pressure from sodium metal. Literature procedures were employed to prepare $\text{VCl}_3(\text{THF})_3$,¹⁷ $\text{V}(\text{C}_{10}\text{H}_8)_2$ (**1a**),¹⁸ $\text{V}(\text{CO})_6$,¹⁹ $\text{Cr}(\text{CNXyl})_6$ (**6**),²⁰ and CsC_8 .²¹ Other reagents were obtained from commercial sources and were freed of oxygen and moisture before use.

Solution infrared spectra were recorded on a Mattson Galaxy 6021 FTIR spectrometer with samples sealed in 0.1 mm gastight CaF_2 cells. Nujol (mineral oil) mulls of all products for IR spectra were prepared in a Vacuum Atmospheres Corp. drybox. NMR samples were sealed under argon into 5 mm tubes and were analyzed on a Varian Unity-300 spectrometer. ¹H and ¹³C chemical shifts are given with reference to residual ¹H and ¹³C solvent resonances relative to TMS. Such referencing eliminated bulk susceptibility effects for paramagnetic samples.²² ¹⁹F and ³¹P chemical shifts are reported relative to *external* CFCl_3 and 85% H_3PO_4 , respectively. In the variable-temperature NMR studies, samples were allowed to equilibrate for at least 20 min at a given temperature prior to data acquisition. The temperature indicated by the console was checked using known temperature dependence of the peak separation of methanol.²³ Solutions for ESR experiments were prepared in the drybox and placed in quartz tubes sealed with septa and Parafilm. The data were recorded using an IBM-Bruker ESP-300 spectrometer. A small Dewar flask was inserted into the microwave cavity to obtain measurements at the liquid N_2 temperature. ESR spectra were referenced to the standard DPPH, 2,2-bis(4-*tert*-octylphenyl)-1-picrylhydrazyl ($g = 2.0036$ at 25 °C). Melting points are uncorrected and were determined for samples in sealed under argon capillaries on a Thomas-Hoover Unimelt apparatus. Microanalyses were carried out by H. Malissa and G. Reuter Analytische Laboratorien, Lindlar, Germany.

Magnetic Susceptibility Measurements. Solid-state volume magnetic susceptibilities were measured on a Johnson Matthey MSB-AUTO balance at ambient temperature and converted into the corresponding molar susceptibilities in the usual way.²⁴ Air-sensitive samples were packed into stoppered gastight tubes (0.400 cm o.d. \times 0.324 cm i.d.) to a depth of ca. 3.0 cm in the drybox. The air correction of 0.029×10^{-6} was applied to volume susceptibilities of the samples packed under argon. Diamagnetic corrections, applied to the molar susceptibilities of the paramagnetic substances, are reported as χ_{diam} . The latter corrections were obtained experimentally and/or were calculated using the standard Pascal's constants.²⁴ The molar susceptibilities of pure 2,6-dimethylphenyl isocyanide, CNXyl, and $\text{Cr}(\text{CNXyl})_6$ were measured to be -71.6×10^{-6} and $-452.3 \times 10^{-6} \text{ cm}^3 \text{ mol}^{-1}$, respectively. Unless otherwise specified, the effective magnetic moments are reported for solid samples. Solution magnetic susceptibilities were obtained by the

(16) (a) Shriver, D. F.; Drezdon, M. A. *The Manipulation of Air-Sensitive Compounds*, 2nd ed.; Wiley-Interscience: New York, 1986. (b) Ellis, J. E. *ACS Symp. Ser.* **1987**, *357*, 34.

(17) Manzer, L. E. *Inorg. Synth.* **1982**, *21*, 135.

(18) Pomije, M. K.; Kurth, C. J.; Ellis, J. E.; Barybin, M. V. *Organometallics* **1997**, *16*, 3582.

(19) Ellis, J. E.; Faltynek, R. A.; Rochfort, G. L.; Stevens, R. E.; Zank, G. A. *Inorg. Chem.* **1980**, *19*, 1082.

(20) Yamamoto, Y.; Yamazaki, H. *J. Organomet. Chem.* **1985**, *282*, 191.

(21) Bergbreiter, D. E.; Killough, J. M. *J. Am. Chem. Soc.* **1978**, *100*, 2126.

(22) La Mar, G. N.; Horrocks, W. D., Jr.; Holm, R. H., Eds. *NMR of Paramagnetic Molecules*; Academic Press: New York, 1973.

(23) (a) Van Geet, A. *Anal. Chem.* **1970**, *42*, 679. (b) Van Geet, A. *Anal. Chem.* **1968**, *40*, 2227.

(24) (a) Earnshaw, A. *Introduction to Magnetochemistry*; Academic Press: New York, 1968. (b) Kahn, O. *Molecular Magnetism*; VCH Publishers: New York, 1993.

Evans method²⁵ on a Varian Unity 300 instrument at 23 °C. The difference in the solution and solvent densities was disregarded, as usual.²³ Mass susceptibilities of pure solvents were either measured on the Johnson Matthey MSB-AUTO balance or taken from a literature source.²⁶

Synthesis of V(C₁₀H₇Me)₂ (1b). A deep green solution of NaC₁₀H₇-Me was prepared by transferring a solution of 1-methylnaphthalene (84 mmol, 12 mL) in 200 mL of THF into a flask containing sodium metal (65.3 mmol, 1.50 g), cut into ca. 20 small pieces, and a large glass covered magnetic stir bar. After being stirred for 5 h in the dark at room temperature, the mixture was cooled to -55 °C. Then a cold (-55 °C) solution/slurry of VCl₃(THF)₃ (16.1 mmol, 6.00 g) in 150 mL of THF was added via cannula to the cold NaC₁₀H₇Me solution. The resulting brown mixture was slowly warmed to room temperature for 15 h with constant stirring. Subsequently, the mixture was cooled to 0 °C. Alumina (45 g) was added by a bent Schlenk tube at 0 °C over a period of 10 min to give a dark red slurry. This slurry was vigorously stirred for 2 h at 0 °C and then filtered through a 3 cm column of alumina. The filter cake was washed with additional THF until the washings were colorless. All THF was removed in vacuo from the deep maroon-red filtrate, giving a red-brown solution/slurry of V(C₁₀H₇Me)₂ in 1-methylnaphthalene. The excess ligand was carefully removed by short-path distillation (10⁻² Torr, 40–50 °C). The brown residue was recrystallized from toluene/pentane at -78 °C, resulting in a 43% yield of finely divided dark brown **1b** (6.95 mmol, 2.33 g). Anal. Calcd for C₂₂H₂₀V: C, 78.80; H, 6.01. Found: C, 78.25; H, 5.86. $\mu_{\text{eff}}(24\text{ }^\circ\text{C}) = 1.69\ \mu_{\text{B}}$ ($\chi_{\text{diam}} = -219 \times 10^{-6}\ \text{cm}^3\ \text{mol}^{-1}$).

Synthesis of V(CNXYl)₆ (2). A clear ice-cold solution of 2,6-dimethylphenyl isocyanide(CNXYl, 46.6 mmol, 6.11 g) in heptane/THF (70 mL/30 mL) was added to an ice-cold solution of **1b** (6.62 mmol, 2.22 g) in heptane/THF (130 mL/130 mL) via cannula. The reaction mixture changed from a dark red-brown to a deep purple during the addition. The mixture was stirred for 15 h while slowly warming to room temperature. Ca. 150 mL of the solvent was removed in vacuo, resulting in a dichroic green-purple microcrystalline precipitate. The solid was filtered off, washed with pentane (3 × 20 mL), and dried in vacuo. Recrystallization from THF/heptane afforded very air- and moisture-sensitive microcrystalline golden-purple **2** (5.37 mmol, 4.50 g) in an 81% yield. A 91% yield of **2** was obtained using a smaller reaction scale (2.62 mmol, 0.88 g of V(C₁₀H₇Me)₂). Mp: 159–160 °C dec. Anal. Calcd for C₅₄H₅₄N₆V: C, 77.40; H, 6.50; N, 10.03; V, 6.08. Found: C, 77.23; H, 6.52; N, 9.93; V, 6.06. IR (THF): ν_{CN} 2008 w sh, 1939 vs, 1852 w sh cm⁻¹. IR (Nujol mull): ν_{CN} 2006 w sh, 1929 vs br, 1845 m sh cm⁻¹. ¹H NMR (300 MHz, C₆D₅CD₃, 19.9 °C): δ -2.42 (t, ³J_{H-H} = 7.2 Hz, 1H, *p-H*), 9.51 (s, 6H, *o-CH*₃), 13.96 (d, ³J_{H-H} = 7.2 Hz, 2H, *m-H*) ppm. ¹³C{¹H} NMR (75.5 MHz, C₆D₅CD₃, 19.8 °C): δ -93.9 (*W*_{1/2} = 112 Hz, *i-C*), -4.5 (*W*_{1/2} = 8.8 Hz, *o-CH*₃), 101.6 (*W*_{1/2} = 9 Hz, *m-C*), 178.4 (*W*_{1/2} = 21 Hz, *p-C*), 339.0 (*W*_{1/2} = 103 Hz, *o-C*) ppm. $\mu_{\text{eff}}(25\text{ }^\circ\text{C}) = 1.76\ \mu_{\text{B}}$ ($\chi_{\text{diam}} = -452.3 \times 10^{-6}\ \text{cm}^3\ \text{mol}^{-1}$). Substitution of V(C₁₀H₈)₂ (**1a**) for **1b** in the above synthesis resulted in practically identical yields of **2**.

Synthesis of Cs[V(CNXYl)₆] (Cs3). A cold (-50 °C) dark purple solution of **2** (2.36 mmol, 1.980 g) in 250 mL of THF was added to an efficiently stirred cold (-50 °C) orange-brown suspension of excess Cs₈ (4.78 mmol, 1.094 g) in 50 mL of THF via cannula. The reaction turned dark brown and was stirred for ca. 18 h while slowly warming to room temperature. Then the mixture was filtered to give a greenish-black filter cake and a dark brown filtrate. The filter cake was washed with additional THF (ca. 30 mL) until the washings were colorless. Heptane (200 mL) was added to the filtrate and about 300 mL of the solvent was removed in vacuo to afford a microcrystalline brown precipitate, which was filtered off and dried under vacuum. Recrystallization from THF/heptane followed by drying in vacuo for 4 h resulted in an 84% yield (1.99 mmol, 1.930 g) of Cs₃ as an extremely air- and moisture-sensitive microcrystalline bright brown solid. Anal. Calcd for C₅₄H₅₄N₆CsV: C, 66.80; H, 5.61; N, 8.66. Found: C, 66.47;

H, 5.43; N, 8.76. IR (THF): ν_{CN} 2028 vw br, 1823 vs br, 1772 sh br cm⁻¹. IR (Nujol mull): ν_{CN} 1999 vw, 1856 s sh, 1802 vs br cm⁻¹. ¹H NMR (300 MHz, CD₃CN, 25 °C): δ 2.39 (s, 6H, *o-CH*₃), 6.69 (t, ³J_{H-H} = 7.5 Hz, 1H, *p-H*), 6.90 (d, ³J_{H-H} = 7.5 Hz, 2H, *m-H*) ppm. ¹³C{¹H} NMR (75.5 MHz, CD₃CN, 25 °C): δ 20.3 (*o-CH*₃), 122.9 (*p-C*), 128.5 (*m-C*), 133.2 (*o-C*) ppm.

Synthesis of [Cs(18-Crown-6)₂]3**.** A cold (-60 °C) solution of 18-Crown-6 (3.78 mmol, 1.00 g) in 60 mL of THF was transferred into a flask containing a cold (-60 °C) solution of Cs₃ (1.03 mmol, 1.00 g) in 100 mL of THF via cannula. The reaction turned deep purple-violet and was stirred for ca. 15 h while slowly warming to room temperature. An additional 50 mL of THF was used to completely dissolve a small amount of green microcrystalline precipitate formed and the mixture was filtered through a medium porosity frit. Heptane (100 mL) was added to the filtrate and about 130 mL of the solvent was removed in vacuo to give a dichroic green-violet precipitate. The solid was filtered off, washed with pentane (5 × 30 mL), and dried under vacuum. Recrystallization from THF/pentane followed by drying in vacuo for 18 h (important!) afforded [Cs(18-Crown-6)₂]**3** (0.90 mmol, 1.350 g) in an 87% yield as a finely divided dark amber microcrystalline solid. Mp: 193–195 °C dec. Anal. Calcd for C₇₈H₁₀₂N₆CsO₁₂V: C, 62.48; H, 6.86; N, 5.60. Found: C, 62.29; H, 6.74; N, 5.71. IR (THF): ν_{CN} 2021 vw br, 1872 s sh, 1818 vs br, ν_{CO} 1113 s cm⁻¹. IR (Nujol mull): ν_{CN} 2021 vw, 1874 s sh, 1801 vs br, ν_{CO} 1111 s cm⁻¹. ¹H NMR (300 MHz, CD₃CN, 25 °C): δ 2.41 (s, 6H, *o-CH*₃), 3.51 (s, 8H, 18-C-6), 6.66 (t, ³J_{H-H} = 7.5 Hz, 1H, *p-H*), 6.92 (d, ³J_{H-H} = 7.5 Hz, 2H, *m-H*) ppm. ¹³C{¹H} NMR (75.5 MHz, CD₃CN, 25 °C): δ 20.3 (*o-CH*₃), 71.2 (*18-C-6*), 122.9 (*p-C*), 128.4 (*m-C*), 133.8 (*o-C*) ppm.

Synthesis of [K(Crypt{2.2.2})]3**.** A cold solution of **2** (1.19 mmol, 1.000 g) in 50 mL of THF was rapidly added to a cold green solution/slurry of [K(Crypt{2.2.2})][C₁₀H₈] at -70 °C. The latter was prepared by stirring potassium metal (1.20 mmol, 0.047 g), naphthalene (2.42 mmol, 0.310 g), and Cryptand{2.2.2} in 50 mL of THF for 4 h. The reaction mixture turned dark violet and was stirred for 15 h while slowly warming to room temperature. A green microcrystalline precipitate formed. The mixture was filtered to provide an iridescent green solid. The solid was washed with THF (150 mL), pentane (5 × 15 mL), and ether (3 × 30 mL) and dried in vacuo for 4 h to afford free green microcrystalline [K(Crypt{2.2.2})]**3** (1.14 mmol, 1.430 g) in a 96% yield. Mp: 238–239 °C dec, darkens at 230 °C. IR (HMPA): ν_{CN} 2022 vw br, 1998 vw br, 1874 s sh, 1810 vs br cm⁻¹. IR (Nujol mull): ν_{CN} 2022 vw, 1999 vw, 1875 s sh, 1764 vs br cm⁻¹.

Reaction of Cs₃ with [Et₃NH]Cl. A cold (-60 °C) dark brown solution of Cs₃ (0.515 mmol, 0.500 g) in 60 mL of THF was rapidly transferred into a flask containing a cold (-60 °C) suspension of [Et₃NH]Cl (0.515 mmol, 0.071 g) in 20 mL of THF. The mixture turned deep purple within 2 h of stirring at -60 °C. Then the reaction was warmed to room temperature and the mixture was filtered. Heptane (100 mL) was added to the filtrate, which was concentrated to about 20 mL to give a green-purple precipitate. The solid was filtered off, washed with pentane (2 × 10 mL), and dried under vacuum for 2 h to give a 75% yield of the product (0.388 mmol, 0.325 g), which was spectroscopically (IR) and magnetically identical with genuine **2**.

Synthesis of [V(CNXYl)₆][PF₆]₄ (4[PF₆]). A cold (-70 °C) solution of **2** (1.07 mmol, 0.900 g) in 80 mL of THF was transferred to a cold (-70 °C) suspension of [Cp₂Fe][PF₆] (1.07 mmol, 0.357 g) in 20 mL of THF. The reaction mixture turned deep orange-red and was stirred for 15 h while slowly warming to room temperature. Heptane (70 mL) was introduced into the reaction flask and ca. 85 mL of the solvent was removed in vacuo to give a deep red microcrystalline precipitate. The solid was filtered off, washed with pentane (3 × 20 mL) until the washings were colorless, and dried in vacuo. Recrystallization from THF/pentane followed by drying in vacuo for 3 h afforded dark red microcrystalline 4[PF₆] (0.99 mmol, 0.972 g) in a 92% yield. Mp: 179–181 °C dec, darkens at 150 °C. Anal. Calcd for C₅₄H₅₄N₆F₆PV: C, 65.98; H, 5.54; N, 8.55. Found: C, 65.71; H, 5.48; N, 8.40. IR (THF): ν_{CN} 2142 w, 2033 vs, 1995 m, ν_{PF} 844 vs cm⁻¹. IR (Nujol mull): ν_{CN} 2143 w, 2107 m sh, 2018 vs br, 1984 s, ν_{PF} 840 vs cm⁻¹. ¹H NMR (300 MHz, THF-*d*⁸, 22 °C): δ 2.35 (s, 6H, *o-CH*₃), 7.13 (s br, 3H, *m*- and *p-H*) ppm. ¹³C{¹H} NMR (75.5 MHz, THF-*d*⁸, 22 °C): δ 19.0 (*o-CH*₃), 129.1 (*p-C*), 129.2 (*m-C*), 129.3 (*i-C*), 134.2 (*o-C*) ppm. ³¹P

(25) (a) Evans, D. F. *J. Chem. Soc.* **1959**, 2003. (b) Crawford, T. H.; Swanson, J. J. *J. Chem. Educ.* **1971**, *48*, 382. (c) Sur, S. K. *J. Magn. Reson.* **1989**, *82*, 169.

(26) Weast, R. C., Ed. *Handbook of Chemistry and Physics*; CRC Press: Cleveland, OH, 1976.

NMR (121.4 MHz, THF- d_6 , 21 °C): δ -142.9 (septet, $^1J_{P-F} = 709$ Hz) ppm. ^{19}F NMR (282.2 MHz, THF- d_6 , 21 °C): δ -74.35 (d, $^1J_{F-P} = 710$ Hz) ppm. $\mu_{\text{eff}}(24 \text{ °C}) = 2.74 \mu_B$ ($\chi_{\text{diam}} = -519.3 \times 10^{-6} \text{ cm}^3 \text{ mol}^{-1}$).

Synthesis of trans-V(CO)₂(CNXyl)₄ (5). A solution of V(CO)₆ (2.28 mmol, 0.500 g) in 150 mL of heptane was added to a solution of 2,6-dimethylphenyl isocyanide (16.01 mmol, 2.100 g) in 100 mL of heptane at room temperature in a flask open to a mercury bubbler. The reaction rapidly changed from a yellow-green color of V(CO)₆ to an orange and then to an orange-brown. An extensive gas evolution was observed. In about 7 h, a deep red solution/slurry formed. The mixture was allowed to stir in the dark for a total of 72 h at room temperature. All but 40 mL of heptane was removed in vacuo and the slurry was filtered to collect a bright red solid, which was washed thoroughly with pentane (5 × 15 mL) until the washings were pale orange and dried under vacuum. This solid was redissolved in 150 mL of toluene to give a deep orange-red solution and filtered. Removal of all toluene from the filtrate and recrystallization from THF/heptane afforded lustrous deep mulberry, microcrystalline **5** (1.82 mmol, 1.150 g) in an 80% yield. Compound **5** decomposed without melting above ca. 100 °C to a black material. Anal. Calcd for C₃₈H₃₆N₄O₂V: C, 72.26; H, 5.74; N, 8.87. Found: C, 71.93; H, 5.76; N, 8.93. IR (toluene): ν_{CN} 2011 m, 1984 vs, ν_{CO} 1889 w br, 1840 vs cm^{-1} . IR (Nujol mull): ν_{CN} 2011 m, 1986 vs, ν_{CO} 1897 vw, 1808 vs cm^{-1} . $\mu_{\text{eff}}(22 \text{ °C}) = 1.75 \mu_B$ ($\chi_{\text{diam}} = -336.2 \times 10^{-6} \text{ cm}^3 \text{ mol}^{-1}$). ESR (5mM solution in toluene glass, -196 °C): $g_{\text{av}} = 2.023$ ($g_{\perp} = 2.038$, $g_{\parallel} = 1.993$); $A_{\text{av}} = 47$ G ($A_{\perp} = 31$ G, $A_{\parallel} = 80$ G).

Oxidation of 5 with [Cp₂Fe]⁺ in the Presence of CNXyl. A solution of **5** (0.791 mmol, 0.500 g) and CNXyl (2.371 mmol, 0.311 g) in 60 mL of THF was transferred to a suspension of [Cp₂Fe][PF₆] in 10 mL of THF at 0 °C. A moderate gas evolution was observed. The mixture was stirred for 15 h while slowly warming to room temperature. The resulting deep orange solution was filtered and the filtrate was concentrated to ca. 20 mL. Addition of heptane (100 mL) produced a deep red precipitate and an orange solution. The solid was filtered off, washed with pentane (4 × 15 mL), and dried under vacuum to afford an 80% yield of free flowing dark red **3**[PF₆], which was identical with the bona fide [V(CNXyl)₆][PF₆].

Synthesis of [Cr(CNXyl)₆][BF₄] (7[BF₄]). Microcrystalline golden-yellow **7**[BF₄] was isolated in a 91% yield by oxidizing Cr(CNXyl)₆ (**6**) with 1 equiv of Ag[BF₄] in O₂-free acetone.²⁷ This procedure is a variation of the method established by Treichel and Essenschmayer to prepare other Cr(1+) aryl isocyanide complexes.²⁸ Mp: 190–192 °C. IR (THF): ν_{CN} 2055 vs, 1996 w sh cm^{-1} . 1H NMR (300 MHz, CDCl₃, 19.9 °C): δ -1.48 (t, $^3J_{H-H} = 7.5$ Hz, 1H, *p-H*), 8.74 (s, 6H, *o-CH₃*), 12.53 (d, $^3J_{H-H} = 7.5$ Hz, 2H, *m-H*) ppm. $^{13}C\{^1H\}$ NMR (75.5 MHz, CDCl₃, 19.9 °C): δ -32.9 ($W_{1/2} = 50$ Hz, *i-C*), -0.8 ($W_{1/2} = 6$ Hz, *o-CH₃*), 90.6 ($W_{1/2} = 12$ Hz, *m-C*), 179.6 ($W_{1/2} = 16$ Hz, *p-C*), 224.2 ($W_{1/2} = 28$ Hz, *o-C*) ppm. $\mu_{\text{eff}}(26 \text{ °C}) = 1.92 \mu_B$ ($\chi_{\text{diam}} = -491.3 \times 10^{-6} \text{ cm}^3 \text{ mol}^{-1}$). Magnetic and spectroscopic properties of this substance are fully in accord with the assigned formulation.

Synthesis of [Cr(CNXyl)₆][PF₆]₂ (8[PF₆]₂). Microcrystalline yellow-orange **8**[PF₆]₂ was isolated in a 73% yield by oxidizing **6** with 2 equiv of Ag[PF₆] in CH₂Cl₂.²⁷ This synthesis is based on the procedure established for the preparation of other Cr(2+) aryl isocyanides.²⁸ Mp: 242–244 °C dec, darkens at 218 °C. IR (CH₂Cl₂): ν_{CN} 2140 vs cm^{-1} . IR (Nujol mull): ν_{CN} 2152 vs sh, 2138 vs, 1962 vw cm^{-1} . 1H NMR (300 MHz, CD₂Cl₂, 21.0 °C): δ -15.87 (s, br, 1H, *p-H*), 19.06 (d, $^3J_{H-H} = 6.9$ Hz, 2H, *m-H*), 19.10 (s, 6H, *o-CH₃*) ppm. 1H NMR (300 MHz, CD₂Cl₂, -63.5 °C): δ -26.51 (s, br, 1H, *p-H*), 23.94 (s, br, 2H, *m-H*), 26.60 (s, br, 6H, *o-CH₃*) ppm. ^{31}P NMR (121.4 MHz, CD₂Cl₂, 21.0 °C): δ -143.3 (septet, $^1J_{P-F} = 711$ Hz) ppm. ^{19}F NMR (282.2 MHz, CD₂Cl₂, 21.0 °C): δ -73.88 (d, $^1J_{F-P} = 711$ Hz) ppm. $\mu_{\text{eff}}(26 \text{ °C}) = 3.02 \mu_B$ ($\chi_{\text{diam}} = -586 \times 10^{-6} \text{ cm}^3 \text{ mol}^{-1}$). Magnetic and spectroscopic properties of this substance are fully consistent with the assigned formulation.

X-ray Crystallographic Characterization of 2, Cs3, 4[PF₆], and 5. X-ray quality crystals of **2**, **4**[PF₆] \cdot THF, and **5** were grown by

carefully layering cold (0 °C) pentane over a cold (0 °C) THF solution of the appropriate compound. Crystals of Cs**3** were obtained by layering cold (0 °C) pentane over a cold (0 °C) DME solution of Cs**3**. All manipulations with the crystals prior to transfer to the goniometer were performed in an argon filled glovebag to protect the samples from the atmosphere. A selected crystal was coated with viscous oil, attached to a glass fiber, and mounted on the Siemens SMART Platform CCD diffractometer for a data collection (Mo K α radiation with $\lambda = 0.71073$ Å was employed). An initial set of cell constants was calculated from reflections harvested from three sets of 20 frames. These initial sets of frames were oriented such that orthogonal wedges of reciprocal space were surveyed. Final cell constants were calculated from the actual data collection. During the data collection a randomly oriented region of reciprocal space was surveyed to the extent of 1.3 hemispheres to a resolution of 0.84 Å. Three major swaths of frames were collected with 0.30° steps in ω . Space groups were determined based on systematic absences and intensity statistics. Successful direct-methods solutions were calculated, which provided most non-hydrogen atoms from the *E*-maps. Several full-matrix least squares/difference Fourier cycles were performed to locate the remainder of the non-hydrogen atoms. All non-hydrogen atoms were refined anisotropically. All hydrogen atoms were placed in ideal positions and refined as riding atoms with individual or group isotropic displacement parameters. For Cs**3**, one relatively large difference peak (2.39 e Å⁻³) was found near Cs(2). This peak appears to be spurious. For **5**, there were two space groups available, *P4nc* and *P4/mnc* in Laue class *4/mmm*. The mean $|E^2 - 1| = 0.809$ favored the noncentrosymmetric space group *P4nc*.²⁹ The Flack absolute structure parameter, *x*, of 0.01(3) indicated³⁰ that the specimen was enantiomerically pure and its absolute configuration was chosen correctly. All calculations were performed on SGI INDY R4400-SC or Pentium computers using the SHELXTL V5.0 suite of programs (SHELXTL-Plus V5.0, Siemens Industrial Automation, Inc, Madison, WI). For all structures, the program SADABS was used to correct the data for absorption. The program PLATON/SQUEEZE³¹ was employed to take into account the effects of disordered solvent in the cases of Cs**3** and **4**[PF₆] \cdot THF. Crystal data, data collection, solution, and refinement information for **2**, Cs**3**, **4**[PF₆] \cdot THF, and **5** is provided in Table 1. Additional crystallographic details can be found in the Supporting Information.

Results and Discussion

Synthetic Work. Recently, we have established a conventional synthesis of bis(naphthalene)vanadium(0), V(C₁₀H₈)₂ (**1a**).¹⁸ This undeservedly forgotten³² substance reacted smoothly with carbon monoxide under very mild conditions to afford V(CO)₆,¹⁸ and, therefore, seemed to be a very promising labile precursor to other compounds of zerovalent vanadium. Because of the rather modest yields (14–29%) obtained in the preparation of **1a**,^{18,27} synthesis of its methylated derivative, bis(1-methylnaphthalene)vanadium(0), V(C₁₀H₇Me)₂ (**1b**), was attempted in hopes of a more efficient generation of a synthon for low-spin atomic vanadium. Thus, “overreduction” of VCl₃(THF)₃ with 4 equiv of NaC₁₀H₇Me at -55 °C,¹⁸ followed by addition of alumina, provided a dark red solution from which pure dark brown **1b** was reproducibly isolated in a 43% yield. The substantially better yield of **1b** (43%) compared to that of **1a** (14%) under identical experimental conditions (magnetic stirring) may be attributed to a greater solubility of NaC₁₀H₇Me vs NaC₁₀H₈ in THF at low temperature. The above facile synthesis of **1b** compares favorably with Timms’ original

(29) Stout, G. H.; Jensen, L. H. *X-ray Structure Determination*; John Wiley & Sons: New York, 1989.

(30) Flack, H. D. *Acta Crystallogr.* **1983**, A39, 876.

(31) Spek, A. L. *Acta Crystallogr.* **1990**, A46, C34.

(32) Complex **1a** was originally isolated by Küding and Timms by condensing vanadium atoms in a cold methylcyclohexane/THF solution of naphthalene (Küding, E. P.; Timms, P. L. *J. Chem. Soc., Chem. Commun.* **1977**, 912). However, the yield of **1a** was not specified and no chemical properties of this substance were reported prior to our¹⁸ recent study.

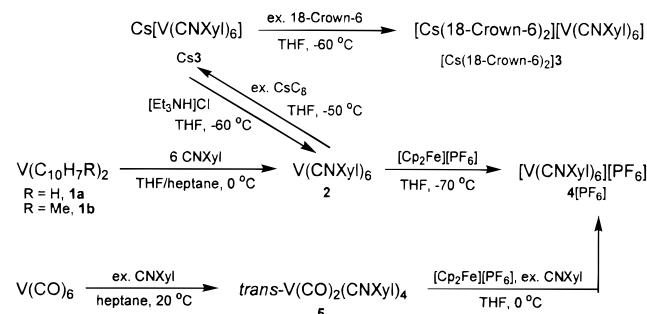
(27) Barybin, M. V. Ph.D. Dissertation, University of Minnesota, 1999.

(28) Treichel, P. M.; Essenschmayer, G. P. *Inorg. Chem.* **1976**, 15, 146.

Table 1. Crystal Data, Data Collection, Solution, and Refinement for **2**, Cs**3**, **4**[PF₆]₃·THF, and **5**

	2	Cs 3	4 [PF ₆] ₃ ·THF	5
empirical formula	C ₅₄ H ₅₄ N ₆ V	C ₅₄ H ₅₄ C ₈ N ₆ V	C ₅₈ H ₆₂ N ₆ OPV	C ₃₈ H ₃₆ N ₄ O ₂ V
formula weight	837.97	970.88	1055.05	631.65
crystal habit, color	plate, deep purple	block, green-purple	irregular block, red	block, red
crystal size (mm)	0.22 × 0.22 × 0.10	0.45 × 0.35 × 0.30	0.40 × 0.32 × 0.23	0.36 × 0.25 × 0.14
crystal system	triclinic	triclinic	monoclinic	tetragonal
space group	<i>P</i> $\bar{1}$	<i>P</i> $\bar{1}$	<i>P</i> ₂ / <i>c</i>	<i>P</i> 4 <i>nc</i>
<i>a</i> (Å)	10.7588(3)	12.0077(2)	15.6942(4)	13.7245(1)
<i>b</i> (Å)	11.2539(2)	14.3698(1)	20.8924(6)	13.7245(1)
<i>c</i> (Å)	11.8350(3)	17.1379(2)	19.6343(5)	9.1904(1)
α (deg)	117.760(1)	66.534(1)	90	90
β (deg)	109.184(1)	79.878(1)	98.749(1)	90
γ (deg)	92.153(2)	83.106(1)	90	90
<i>V</i> (Å ³)	1166.05(5)	2666.23(5)	6363.0(3)	1731.12(3)
<i>Z</i>	1	2	4	2
ρ_{calc} (Mg m ⁻³)	1.193	1.209	1.101	1.212
μ (mm ⁻¹)	0.255	0.897	0.237	0.324
<i>F</i> (000)	443	996	2208	662
temp (K)	173(2)	173(2)	173(2)	153(2)
θ range (deg)	2.06–24.97	1.31–25.00	1.31–25.03	2.10–24.99
index range	–12 ≤ <i>h</i> ≤ 11 –13 ≤ <i>k</i> ≤ 11 0 ≤ <i>l</i> ≤ 14	–13 ≤ <i>h</i> ≤ 14 –15 ≤ <i>k</i> ≤ 17 0 ≤ <i>l</i> ≤ 20	–18 ≤ <i>h</i> ≤ 18 0 ≤ <i>k</i> ≤ 24 0 ≤ <i>l</i> ≤ 23	0 ≤ <i>h</i> ≤ 11 0 ≤ <i>k</i> ≤ 16 –10 ≤ <i>l</i> ≤ 8
no. of rflns collected	6555	15296	30108	8539
no. of unique rflns	3941	9071	11001	1379
<i>R</i> _{int} ^a	0.0335	0.0184	0.0360	0.0248
max/min transmission	1.0000/0.6986	1.000/0.809	1.000/0.806	1.000/0.892
data/restraints/params	3941/0/283	9067/0/565	10998/35/670	1379/1/108
no. of rflns with <i>I</i> > 2 σ (<i>I</i>)	2522	7740	6612	1313
<i>RI</i> ; ^b <i>wR2</i> ^c (<i>I</i> > 2 σ (<i>I</i>))	0.0630; 0.1216	0.0524; 0.1568	0.0658; 0.1628	0.0253; 0.0640
GOF on <i>F</i> ²	1.01	1.02	1.067	1.150
largest diff peak/hole (e Å ⁻³)	0.263/–0.370	2.394/–0.507	0.554/–0.321	0.140/–0.220

$$^a R_{\text{int}} = \sum |F_o^2 - \langle F_c^2 \rangle| / \sum |F_o^2|. \quad ^b RI = \sum ||F_o| - |F_c|| / \sum |F_o|. \quad ^c wR2 = [\sum (w(F_o^2 - F_c^2)^2) / \sum (w(F_o^2)^2)]^{1/2}.$$

Scheme 1

preparation of this compound involving condensation of potassium atoms into a solution of VCl₃ and C₁₀H₇Me in THF at –100 °C.³³ The latter provided a 25% yield of **1b**, which presumably exists as a mixture of several isomers.³³ Both **1a** and **1b** proved to be essential for establishing the isocyanide chemistry of low-valent vanadium summarized in Scheme 1.

V(CNXyl)₆ (2). In a typical synthesis of **2**, a slight excess (7 equiv) of 2,6-dimethylphenyl isocyanide, was reacted with **1b** in THF/heptane at 0 °C. The red-brown color of **1b** rapidly changed to a deep purple. After the reaction had been completed, most of the THF was removed in vacuo to give beautiful dichroic green-purple microcrystals and a deep purple solution. Workup and recrystallization afforded analytically pure microcrystalline golden-purple **2** in 81–91% yields (Scheme 1). The use of **1a** instead of **1b** in the above procedure worked equally well. The remarkably clean substitution of the naphthalene ligands from **1a,b** by CNXyl nicely demonstrates the so-called “naphthalene effect”³⁴ exhibited by the V(C₁₀H₇R)₂ complexes.

(33) (a) Hawker, P. N.; Kündig, E. P.; Timms, P. L. *J. Chem. Soc., Chem. Commun.* **1978**, 730. (b) Hawker, P. N.; Timms, P. L. *J. Chem. Soc., Dalton Trans.* **1983**, 1123.

Compound **2** is stable at room temperature both in the solid state and in solution (THF, benzene, toluene) under argon. However, this complex is very air- and moisture-sensitive. Indeed, deep purple solutions of **2** decolorized within seconds upon exposure to atmospheric air to give free CNXyl and uncharacterized yellow-brown decomposition product(s).

Compound **2** is the first vanadium(0) complex to contain an isocyanide ligand and may be considered an analogue of the long-established V(CO)₆.³⁵ It is well-known that V(CO)₆ undergoes rapid disproportionation in THF.³⁶ On the contrary, **2** is perfectly stable in this solvent for weeks at room temperature. While V(CO)₆ is easily reduced by cobaltocene and decamethylcobaltocene to give [V(CO)₆][–],³⁷ **2** is unreactive toward these substances. The latter fact is in accord with CO being a better π -acceptor than CNXyl. Solution and Nujol mull infrared spectra of **2** in the ν_{CN} stretching region resemble those reported for the analogous octahedral Cr(0) complex, Cr(CNXyl)₆.^{20,38} The frequency of the most intense peak is depressed by 178 cm^{–1} compared to ν_{CN} found for free CNXyl (2117 cm^{–1} in THF) indicating a significant degree of back-bonding within **2**. Similarly, ν_{CO} of V(CO)₆ is about 170 cm^{–1} lower in energy than that of free CO.³⁵

The bulky nature of the 2,6-xylyl isocyanide (vide infra) was essential for the stability of **2**. Indeed, reactions of **1b** with

(34) (a) Kündig, E. P.; Perret, C.; Spichiger, S.; Bernardinelli, G. J.; *Organomet. Chem.* **1985**, 286, 183. (b) Basolo, F. *New J. Chem.* **1994**, 18, 19. (c) Albright, T. A.; Hofmann, P.; Hoffmann, R.; Lillya, C. P.; Dobosh, P. A. *J. Am. Chem. Soc.* **1983**, 105, 3396.

(35) Natta, G.; Ercoli, R.; Calderazzo, F.; Alberola, A.; Corrandini, P.; Allegra, G. *Atti Acad. Naz. Lincei, Classe Sci. Fis. Mater. Nat.* **1959**, 27, 107.

(36) Hieber, W.; Winter, E.; Schubert, E. *Chem. Ber.* **1962**, 95, 196. (37) (a) Calderazzo, F.; Pampaloni, G. *J. Chem. Soc., Chem. Commun.* **1984**, 1249. (b) Calderazzo, F.; Pampaloni, G.; Pelizzi, G.; Vitali, F. *Polyhedron* **1988**, 7, 2039.

(38) Bullock, J. P.; Mann, K. R. *Inorg. Chem.* **1989**, 28, 4006.

excess 4-methylphenyl isocyanide, CNTol, afforded only uncharacterized isocyanide polymerization product(s). The initial product, presumably $V(\text{CNTol})_6$, was stable for short periods of time in THF or toluene solutions below -60°C (IR evidence).²⁷ All attempts to isolate this extremely reactive species failed. Thus, the methyl substituents in the ortho positions of the coordinated aryl isocyanide ligands appear to be absolutely necessary for the stability of $V(\text{CNAr})_6$. Perhaps they effectively shield the $V(\text{CN})_6$ core from an outside attack and/or prevent the ligating carbon atoms from coming too close to each other to ultimately form a C–C bond. Notably, treatment of **1a** or **1b** with a large excess of CN^tBu at low temperature did not yield $V(\text{CN}^t\text{Bu})_6$ and led only to partial decomposition of CN^tBu . This result is in marked contrast with the fact that $\text{Cr}(\text{C}_{10}\text{H}_8)_2$ reacts smoothly with CN^tBu at 0°C to give $\text{Cr}(\text{CN}^t\text{Bu})_6$.³⁹

$[\text{V}(\text{CNXyl})_6]^-$ (**3**). Recently, Cooper and co-workers have isolated the first four- and five-coordinate binary isocyanide metalates, $[\text{Co}(\text{CNXyl})_4]^-$ ^{5,7} and $[\text{Mn}(\text{CNXyl})_5]^-$.⁴⁰ However, due to the well-established tendency of isocyanides to couple in higher coordinate environments, the accessibility of anionic complexes possessing six discrete isocyanide ligands has remained in doubt.⁴⁰ The anion **3**, described below, is the first example of such species.⁴¹ Notably, its carbonyl analogue, $[\text{V}(\text{CO})_6]^-$, has been known for nearly 40 years.⁴²

One-electron reduction of **2** was achieved by stirring its solution in THF with a suspension of excess (2 equiv) cesium graphite, CsC_8 , at -50°C . Workup followed by recrystallization of the obtained brown solid afforded an 84% yield of unsolvated Cs3 as free flowing bright brown microcrystals (Scheme 1). Cs3 is thermally stable in the solid state. Solutions of the product in THF, DME, and CH_3CN did not show signs of decomposition for days when kept under argon at room temperature. However, unlike its isoelectronic analogues $\text{Cr}(\text{CNXyl})_6$ ²⁰ and $[\text{V}(\text{CO})_6]^-$,⁴² Cs3 is *extremely* air- and moisture-sensitive both in solution and in the solid state and requires exceptional care to be isolated as an analytically pure substance.

The vanadate **3** can also be isolated as a $[\text{K}(\text{Crypt}\{2.2.2\})]^+$ salt by reacting **2** with 1 equiv of $[\text{K}(\text{Crypt}\{2.2.2\})][\text{C}_{10}\text{H}_8]$ in THF at low temperature. Unfortunately, this iridescent green microcrystalline substance is virtually insoluble in THF, DME, CH_3CN , and many other solvents. $[\text{K}(\text{Crypt}\{2.2.2\})]\text{3}$ can be dissolved in hexamethylphosphoramide (HMPA) to give dark violet solutions. However, IR spectra of these solutions showed signs of decomposition within several hours of standing at room temperature. Attempts to prepare the unsolvated potassium salt of **3**, analogous to $[\text{K}(\text{Crypt}\{2.2.2\})][\text{Co}(\text{CNXyl})_4]$,⁵ were unsuccessful.²⁷ It is worth mentioning that neither **2** nor **3** could be accessed by reducing $\text{VCl}_3(\text{THF})_3$ with excess sodium amalgam in the presence of xylyl isocyanide,²⁷ even though reactions, similar to this, worked well to prepare related neutral group 6 metal isocyanides, $\text{M}(\text{CNXyl})_6$ ($\text{M} = \text{Cr}, \text{Mo}$).²⁰ Reductions of $\text{VCl}_3(\text{THF})_3$ with 4 equiv of naphthalene or anthracene radical anions followed by treatment with CNXyl led to polymerization of the isocyanide.^{9a,27} The latter procedures, however, were quite efficient in the syntheses of other $[\text{ML}_6]^-$ ($\text{M} = \text{V}, \text{Nb}, \text{Ta}; \text{L} = \text{CO}, \text{PF}_3$)⁴³ and $[\text{Co}(\text{CNXyl})_4]^-$.⁵

In an attempt to generate the hydride $\text{HV}(\text{CNXyl})_6$, analogous to the extremely unstable possible $\text{HV}(\text{CO})_6$,⁴⁴ Cs3 was treated

with $[\text{Et}_3\text{NH}]\text{Cl}$. However, this resulted in oxidation of the vanadate **3** to neutral **2** (Scheme 1), presumably accompanied by the formation of H_2 , Et_3N , and CsCl . Complex Cs3 combined with two molecules of 18-Crown-6 to give dark amber microcrystalline $[\text{Cs}(18\text{-Crown-6})_2]\text{3}$ (Scheme 1). The presence of two 18-Crown-6 units per cesium cation in this compound is not unusual⁴⁵ and was confirmed by elemental analyses and integration of the ^1H NMR resonances for $[\text{Cs}(18\text{-Crown-6})_2]\text{3}$. This substance is reasonably soluble in THF and presently constitutes the only convenient alternative to the parent Cs3 complex. The IR bands in the ν_{CN} region, observed for **3**, are quite broad and similar to those previously reported for $[\text{Co}(\text{CNXyl})_4]^-$, which is believed to be appreciably distorted from its expected tetrahedral symmetry in solution.⁵ The qualitative similarities in the IR spectral signatures of the cobaltate and the vanadate **3** suggest that the geometry of the latter species is not strictly octahedral. Appreciable bending of the isocyanide ligands in this very electron rich molecule (vide infra) is among the factors reducing the ideal octahedral symmetry of **3**.⁴⁶ Using notation for the O_h group,⁴⁷ the bands at 2021, 1872, and 1818 cm^{-1} in the IR spectrum (THF) of $[\text{Cs}(18\text{-Crown-6})_2]\text{3}$ should correspond to A_1 , E_g , and T_{1u} ν_{CN} modes, respectively. Indeed, $(2021^2 - 1872^2)/(1872^2 - 1818^2) = 2.91$, a value very close to the required 3.0.⁴⁸ The most intense ν_{CN} band for **3** is ca. 120 cm^{-1} lower in energy than that for neutral **2**, indicating increase in the extent of back-donation upon reduction of **2**. Employing the Cotton–Kraihanzel approximation,⁴⁸ one can estimate the C–N force constant, k_{CN} , for the isocyanide ligands in $[\text{Cs}(18\text{-Crown-6})_2]\text{3}$ to be about $13.3\text{ mdyn \AA}^{-1}$, while k_{CN} for free CNXyl is ca. $17.1\text{ mdyn \AA}^{-1}$. Similarly, k_{CO} for $[\text{V}(\text{CO})_6]^-$ is only $14.9\text{ mdyn \AA}^{-1}$, as opposed to $k_{\text{CO}} = 18.7\text{ mdyn \AA}^{-1}$ for free carbon monoxide.⁴⁹

$[\text{V}(\text{CNXyl})_6]^+$ (**4**). Oxidation of **2** with 1 equiv of $[\text{Cp}_2\text{Fe}][\text{PF}_6]$ in THF produced an orange-red solution from which a deep red solid was obtained by adding excess heptane. This precipitate was washed with pentane to remove the byproduct, Cp_2Fe , and recrystallized to afford an almost quantitative yield of analytically pure $\text{4}[\text{PF}_6]$, a dark red microcrystalline substance (Scheme 1). Solutions of $\text{4}[\text{PF}_6]$ in THF or CH_2Cl_2 were stable for months at 4°C under argon but deteriorated within minutes upon exposure to air. This compound proved to be moderately air-sensitive in the solid state as well. Infrared data indicated that one of the decomposition pathways of the anion **3** on exposure to air involved sequential oxidation of **3** to **4** ($\text{3} \rightarrow \text{4} \rightarrow$ decomposition products). It is worth noting that cation **4** was also isolated in ca. 70% yields as $[\text{BF}_4]^-$ and $[\text{BPh}_4]^-$

(42) Ercoli, R.; Calderazzo, F.; Alberola, A. *J. Am. Chem. Soc.* **1960**, *82*, 2966.

(43) (a) Barybin, M. V.; Ellis, J. E.; Pomije, M. K.; Tinkham, M. L.; Warnock, G. F. *Inorg. Chem.* **1998**, *37*, 6518. (b) Barybin, M. V.; Pomije, M. K.; Ellis, J. E. *Inorg. Chim. Acta* **1998**, *269*, 58. (c) Ellis, J. E.; Warnock, G. F.; Barybin, M. V.; Pomije, M. K. *Chem. Eur. J.* **1995**, *1*, 521.

(44) (a) Calderazzo, F.; Pampaloni, G.; Vitali, D. *Gazz. Chim. Ital.* **1981**, *111*, 455. (b) Calderazzo, F.; Pampaloni, G.; Lanfranchi, M.; Pelizzi, G. *J. Organomet. Chem.* **1985**, *296*, 1.

(45) Selected examples: (a) Vidal, J. L.; Troup, J. M. *J. Organomet. Chem.* **1981**, *213*, 351. (b) Tinkham, M. L.; Dye, J. L. *J. Am. Chem. Soc.* **1985**, *107*, 6129.

(46) (a) Cotton, F. A.; Zingales, F. *J. Am. Chem. Soc.* **1961**, *83*, 351. (b) Mann, K. R.; Cimolino, M.; Geoffroy, G. L.; Hammond, G. S.; Orio, A. A.; Albertin, G.; Gray, H. B. *Inorg. Chim. Acta* **1976**, *16*, 97.

(47) Strictly speaking, the highest possible symmetry for $[\text{V}(\text{CNXyl})_6]^-$ is T_h , which is a subgroup of O_h . See ref 46b.

(48) Cotton, F. A.; Kraihanzel, C. S. *J. Am. Chem. Soc.* **1962**, *84*, 4432.

(49) (a) Abel, E. W.; McLean, R. A. N.; Tyfield, S. P.; Braterman, P. S.; Walker, A. P.; Hendra, P. J. *J. Mol. Spectrosc.* **1969**, *30*, 29. (b) Dobson, G. R. *Inorg. Chem.* **1965**, *4*, 1673.

(39) Kündig, E. P.; Timms, P. L. *J. Chem. Soc., Dalton Trans.* **1980**, 991.

(40) Utz, T. L.; Leach, P. A.; Geib, S. J.; Cooper, N. J. *Chem. Commun.* **1997**, 847.

(41) Very recently, we have also isolated the tantalum analogue of **3**, $[\text{Ta}(\text{CNXyl})_6]^-$. See ref 9b.

salts by oxidizing **2** with 1 equiv of Ag[BF₄] or Ag[BPh₄], respectively.²⁷ Spectroscopic (IR and NMR) characteristics of **4** were shown to be independent of the counterion.²⁷

Complex **4** is the first homoleptic V(1+) isocyanide. This thermally robust compound may be regarded as an isocyanide analogue of exceedingly unstable [V(CO)₆]⁺.⁵⁰ The most prominent IR ν_{CN} band for cationic **4** in THF occurs 94 cm⁻¹ higher in energy than that for neutral **2**. Nevertheless, this peak is 84 cm⁻¹ below ν_{CN} found for free xylyl isocyanide in the same solvent. Therefore, substantial back-bonding is still present in **4**. Importantly, complex **4** is paramagnetic in the solid state (vide infra) and does not add a seventh CNXyl ligand. In contrast, the Nb and Ta congeners of **4**, [M(CNXyl)₇]⁺, are both diamagnetic and contain seven coordinate metals.^{9b} Most likely, such a difference is a reflection of the smaller size of vanadium compared to those of niobium and tantalum.

trans-V(CO)₂(CNXyl)₄ (5). To this day, direct substitution reactions of V(CO)₆, proceeding without change in the metal oxidation state, have been limited almost exclusively to the syntheses of a few mixed carbonyl–phosphine^{19,51} and carbonyl–phosphite⁵² vanadium(0) derivatives. The potentially diverse carbonyl displacement chemistry of V(CO)₆ has undoubtedly been hampered by its well-documented tendency to disproportionate in the presence of many ligands, including donor solvents.^{53,54}

Given that both **2** and V(CO)₆ are stable under appropriate conditions, a reaction between hexacarbonylvanadium(0) and xylyl isocyanide was investigated. Solutions of V(CO)₆ and excess CNXyl (7 equiv) in heptane were combined at room temperature (Scheme 1). An extensive gas evolution and a series of color changes were observed. After 3 days of stirring, the reaction mixture was concentrated and filtered. The isolated bright red solid was purified to provide an 80% yield of analytically pure lustrous dark red **5**. Unlike V(CO)₆ (but similar to **2**), compound **5** is stable in toluene and THF under argon at room temperature. Complex **4** is very air- and moisture-sensitive both in solution and in the solid state.

Surprisingly, no disproportionation of V(CO)₆ occurred in the above reaction and complex **5** was the only isolated product. Infrared data indicated that shorter reaction times (<72 h) led to incomplete substitution of four carbonyls from V(CO)₆. Stirring the reaction mixture for 4 additional days (for a total of 7 days) at room temperature did not produce any further changes. An attempt to achieve a higher degree of substitution by slowly raising the temperature of the reaction to 80 °C ultimately led to decomposition of **5**. The assignments of the IR spectra of **5** were confirmed by preparing ¹³CO-labeled *trans*-V(¹³CO)₂(CNXyl)₄, **5***. Indeed, the ν_{CN} frequencies for **5** and **5*** are practically identical, whereas the ν¹³CO peaks for **5*** are

(50) (a) Darensbourg, M. Y. *Progr. Inorg. Chem.* **1985**, *33*, 221 and references therein. (b) Kochi, J. K.; Bockman, T. M. *Adv. Organomet. Chem.* **1991**, *33*, 51. (c) Horowitz, C. P.; Shriver, D. F. *Adv. Organomet. Chem.* **1984**, *23*, 219.

(51) (a) Interrante, L. V.; Nelson, G. V. *J. Organomet. Chem.* **1971**, *25*, 153. (b) Behrens, H.; Lutz, K. *Anorg. Allg. Chem.* **1968**, *356*, 225. (c) Hieber, W.; Winter, E. *Chem. Ber.* **1964**, *97*, 1037. (d) Werner, R. P. M. *Naturforsch.* **1961**, *16b*, 477. (e) Hieber, W.; Peterhans, J.; Winter, E. *Chem. Ber.* **1961**, *94*, 4, 2572.

(52) (a) Shi, Q. Z.; Richmond, T. G.; Trogler, W. C.; Basolo, F. *J. Am. Chem. Soc.* **1984**, *106*, 71. (b) Shi, Q. Z.; Richmond, T. G.; Trogler, W. C.; Basolo, F. *J. Am. Chem. Soc.* **1982**, *104*, 4032.

(53) (a) Berno, P.; Gambarotta, S.; Richeson, D. In *Comprehensive Organometallic Chemistry II*; Abel, E. W., Stone, F. G. A., Wilkinson, G., Eds.; Pergamon: New York, 1995; Vol. 4, pp 2–9 and references therein. (b) Connelly, N. G. In *Comprehensive Organometallic Chemistry*; Wilkinson, G., Stone, F. G. A., Abel, E. W., Eds.; Pergamon: New York, 1983; Vol. 3, pp 647–654 and references therein.

(54) Ellis, J. E.; Faltynek, R. A. *J. Organomet. Chem.* **1975**, *93*, 205.

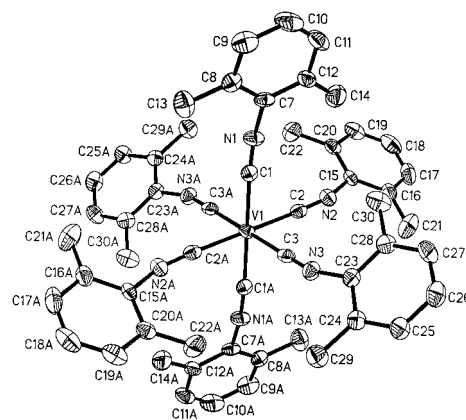


Figure 1. Molecular structure of **2** (50% thermal ellipsoids); hydrogens are omitted for clarity. Selected bond lengths (Å) and angles (deg): V–C1 2.034(3), V–C2 2.022(4), V–C3 2.023(4), C1–N1 1.184(4), C2–N2 1.183(4), C3–N3 1.191(4), C1–N1–C7 168.1(3), C2–N2–C15 158.8(3), C3–N3–C23 161.5(3), av cis C–V–C 90(3), av trans C–V–C 180.0.

shifted as predicted⁵⁵ toward lower energies relative to the corresponding ν¹²CO bands observed for **5**. The presence of two ν_{CN} and two ν_{CO} peaks in the IR spectra of **5** is consistent with the C₄ symmetry of the complex revealed by the X-ray study (vide infra). The higher energy ν_{CO} band is very weak because the corresponding C–O stretching mode is nearly IR-forbidden under the C₄ symmetry. Interestingly, while we observed two relatively sharp ν_{CN} peaks for **5**, Rehder et al. reported a single but broad ν_{CN} band for *trans*-V₁₂(CNXyl)₄.^{10a}

After homoleptic **2**, compound **5** is only the second example of a group 5 metal(0) complex to contain an isocyanide ligand. Displacement of four carbonyls from V(CO)₆ by CNXyl ligands under mild conditions is quite remarkable. The only other known reaction of this type involved interaction of V(CO)₆ with dppe at 120 °C to afford *trans*-V(CO)₂(dppe)₂.^{51b} Although complete carbonyl substitution of V(CO)₆ to give **2** could not be accomplished, oxidation of **5** with 1 equiv of [Cp₂Fe]⁺ in the presence of free CNXyl afforded the binary cationic vanadium isocyanide **4** (Scheme 1).

Structural Characterization of 2–5: V(CNXyl)₆ (2). Complex **2** crystallizes in the space group $\bar{P}1$ with the vanadium atom lying on an inversion center (Figure 1). This results in three independent vanadium–isocyanide units. The molecule is essentially octahedral. The average cis C–V–C angle for **2** is 90(3)° while all trans C–V–C angles are required to be 180° because of the crystallographically imposed symmetry. The structure of **2** exhibits a possible small tetragonal distortion from a regular octahedron, very similar in magnitude to that observed for V(CO)₆.⁵⁶ At the same time, it is 0.07 Å shorter compared to the mean V–C bond in [V(CN^tBu)₆]²⁺ despite a significant

(55) IR for **5***: (toluene) ν_{CN} 2012 s, 1985 vs. ν¹³CO 1844 w br, 1799 vs cm⁻¹; (Nujol mull) ν_{CN} 2015 s, 1988 vs. ν¹³CO 1855 vw, 1768 vs cm⁻¹. Calcd IR ν¹³CO for **5***: (toluene) 1847, 1799 cm⁻¹; (Nujol mull) 1855, 1768 cm⁻¹.

(56) Bellard, S.; Rubinson, K. A.; Sheldrick, G. M. *Acta Crystallogr.* **1979**, *B35*, 271.

(57) Ljungström, E. *Acta Chem. Scand.* **1978**, *A32*, 47.

(58) See Supporting Information for: Lockwood, M. A.; Fanwick, P. E.; Rothwell, I. P. *Organometallics* **1997**, *16*, 3574 (at <http://pubs.acs.org>).

(59) Ericsson, M.-S.; Jagner, S.; Ljungström, E. *Acta Chem. Scand.* **1980**, *A34*, 535.

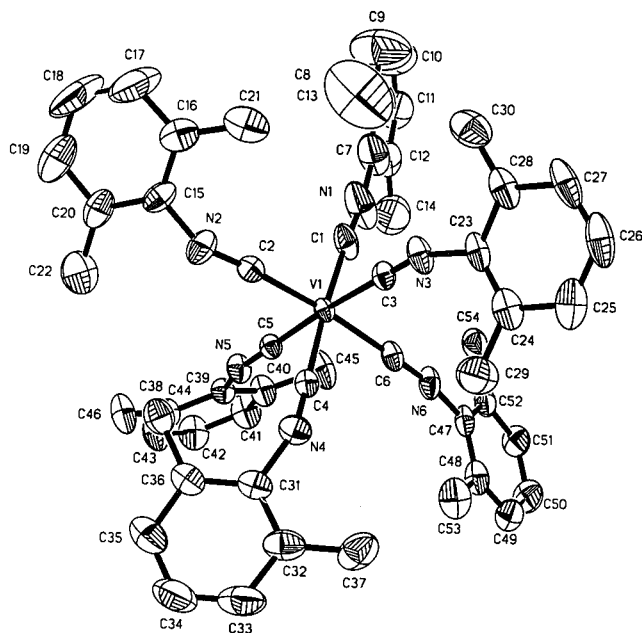


Figure 2. Molecular structure of **3** (50% thermal ellipsoids); hydrogens are omitted for clarity. Selected bond lengths (Å) and angles (deg): V–C1 2.008(4), V–C2 1.939(4), V–C3 1.985(3), V–C4 1.972(4), V–C5 1.986(3), V–C6 2.010(4), C1–N1 1.182(6), C2–N2 1.228(5), C3–N3 1.196(5), C4–N4 1.200(5), C5–N5 1.202(5), C6–N6 1.190(5), C1–N1–C7 166.4(8), C2–N2–C15 145.5(4), C3–N3–C23 157.6(4), C4–N4–C31 148.5(4), C5–N5–C39 158.3(4), C6–N6–C47 170.5(4), av cis C–V–C 90(3), av trans C–V–C 176.0(7).

difference in size of the V(0) and V(2+) ions. In addition, compound **2** possesses relatively long C–NXyl distances (av C–NXyl = 1.186(5) Å) and somewhat bent C–N–Xyl angles (av C–N–Xyl = 163(4)°). All of the above features are consistent with CNXyl functioning as a good π acceptor ligand in **2**. The most noticeable difference between the structures of **2** and $M(\text{CNXyl})_6$ ($M = \text{Mo},^{20} \text{W}^{58}$) is the fact that the trans xylyl rings in **2** are mutually parallel (Figure 1) while these groups in the analogous Mo(0) and W(0) complexes are approximately perpendicular to each other. As in the case of $\text{Mo}(\text{CNXyl})_6$,²⁰ the xylyl substituents in **2** are torsional with respect to the appropriate $\text{V}(\text{CN})_4$ planes. This causes reduction in the overlap between the relevant CN and Xyl π systems. On the contrary, orientation of the phenyl rings in $\text{Cr}(\text{CNPh})_6$ indicates that the CN and phenyl π systems are practically coplanar.⁵⁷ Undoubtedly, the arrangement of the xylyl fragments in **2** is a consequence of balancing electronic and steric factors. The latter constitutes repulsion between methyl substituents of the mutually cis isocyanide ligands. Remarkably, four of the $\text{Me}\cdots\text{Me}$ contacts within **2** are significantly shorter than the doubled van der Waals radius of a methyl group (4.0 Å).

Cs[V(CNXyl)₆] (Cs3). Compound **3** (Figure 2) crystallizes in the space group $P1$ with two anions **3** in the unit cell. One of the cesium counterions, Cs(1), is located on the inversion center ($1/2, 1/2, 1/2$), while the other, Cs(2), is disordered (50:50) over two symmetry related general positions. The $\text{V}(\text{CN})_6$ core is nearly octahedral. All V–C bonds in **3** are statistically shorter than the V–C distances in **2**. This is consistent with the expected increase in back-bonding upon reducing **2** to **3**. Also, as anticipated, the mean V–C distance of 1.98(3) Å in **3** is somewhat longer than that in $[\text{V}(\text{CO})_6]^-$ (1.931(9) Å).⁶⁰ The average C–NXyl bond length of 1.20(2) Å for the vanadate **3** is indistinguishable from analogous values of 1.20(2) and 1.20(3) Å, reported for the only other crystallographically characterized homoleptic isocyanide metalates, $[\text{Mn}(\text{CNXyl})_5]^-$ ⁴⁰ and

Table 2. Close Cs–C and Cs–N Contacts (Å) within Cs3

Cs(1)–C(2)	3.392(3)	Cs(2)–C(1)	3.580(4)
Cs(1)–N(2)	3.417(4)	Cs(2)–N(1)	3.798(4)
Cs(1)–C(3)	3.349(3)	Cs(2)–C(2)	3.426(3)
Cs(1)–N(3)	3.369(3)	Cs(2)–N(2)	3.552(4)
Cs(1)–C(4)	3.506(3)	Cs(2)–C(5)	3.327(3)
Cs(1)–N(4)	3.629(3)	Cs(2)–N(5)	3.375(3)

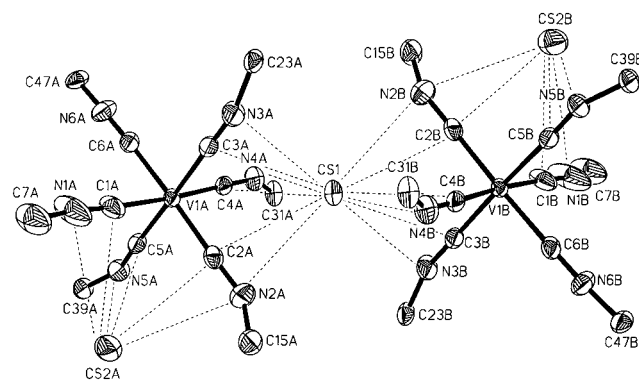


Figure 3. Cation–anion interactions within the unit cell of Cs3; xyllyl substituents are omitted for clarity.

$[\text{Co}(\text{CNXyl})_4]^-$,⁵ respectively. The structure of Cs**3** features rather close contacts between the cesium cations and CN groups of the isocyanide ligands. These are listed in Table 2 and are depicted in Figure 3. Cs(1) is approximately octahedrally coordinated by six CN groups (three from each anion) and may be regarded as a bridge between two vanadate anions. Cs(2) also interacts with three CN fragments of the vanadate.⁶¹ Crystal structures of alkali-metal salts of $[\text{Co}(\text{CNXyl})_4]^-$ ⁵ and certain carbonyl metalates⁶² show similar cation–anion interactions. The large spread in C–N–C angles (and, to a lesser extent, in the structural parameters of the $\text{V}(\text{CN})_6$ core) is undoubtedly a consequence of the described above perturbation of **2** by the cesium counterions. The widest C–N–C angle, C6–N6–C47, of 170.5(4)° corresponds to the isocyanide ligand least affected by the presence of Cs (Figure 3). As in the case of **2**, the bulky nature of CNXyl is likely to be important for the stability of even more electron rich **3**. There are six contacts between methyl substituents within **3** that are shorter than 4.0 Å.

[V(CNXyl)₆][PF₆]⁻ (4[PF₆]). Compound **4**[PF₆] crystallizes in the space group $P2_1/c$ with one ordered and, possibly, one disordered THF molecule in the asymmetric unit. The approximately octahedral geometry of **4** (Figure 4) is relatively unperturbed by the counterion $[\text{PF}_6]^-$ and the solvent of crystallization. The shortest interionic contact of 3.536 Å is between one of the fluorine atoms of $[\text{PF}_6]^-$ and C(30). The mutually trans V–C(3) and V–C(4) bonds are somewhat longer than the other four V–C distances. This may be due to a tetragonal distortion of the low-spin d^4 complex **4**. In **4**, the average V–C bond is 0.04 Å longer while the average C–NXyl bond is 0.02 Å shorter compared to corresponding distances in neutral **2**. Also, the mean C–N–C angle in **4** is 10° greater than that in **2**. All of these facts are consistent with reduction in the extent of back-donation upon proceeding from **2** to **4**. While $\text{Me}\cdots\text{Me}$ contacts within **4** are longer than those within **1** and **2**, six of them are still under 4.0 Å.

(60) Wilson, R. D.; Bau, R. *J. Am. Chem. Soc.* **1974**, *96*, 7601.

(61) Disordered solvent, found in the vicinity of Cs(2), may interact with the Cs(2) cation as well.

(62) (a) Darendbourg, M. Y. *Progr. Inorg. Chem.* **1985**, *33*, 221 and references therein. (b) Kochi, J. K.; Bockman, T. M. *Adv. Organomet. Chem.* **1991**, *33*, 51. (c) Horowitz, C. P.; Shriver, D. F. *Adv. Organomet. Chem.* **1984**, *23*, 219.

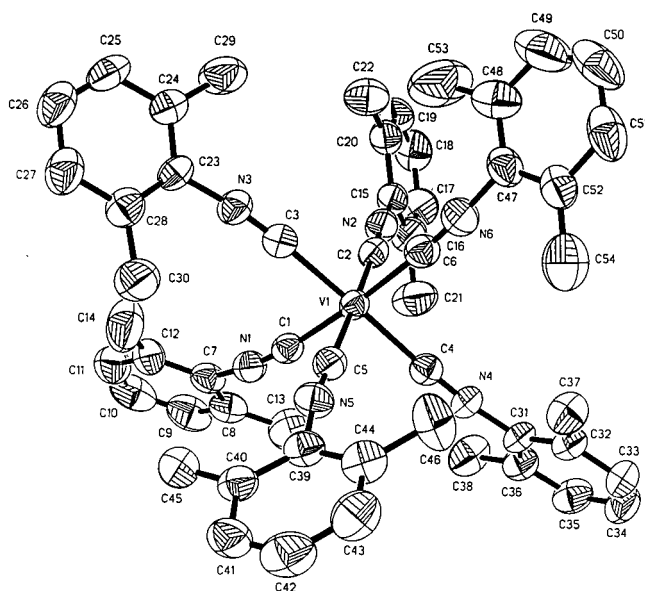


Figure 4. Molecular structure of **4** (50% thermal ellipsoids); hydrogens are omitted for clarity. Selected bond lengths (Å) and angles (deg): V–C1 2.048(4), V–C2 2.062(4), V–C3 2.078(4), V–C4 2.100(4), V–C5 2.061(4), V–C6 2.062(4), C1–N1 1.174(4), C2–N2 1.177(4), C3–N3 1.165(4), C4–N4 1.162(4), C5–N5 1.168(4), C6–N6 1.166(4), C1–N1–C7 170.4(3), C2–N2–C15 176.2(3), C3–N3–C23 173.0(3), C4–N4–C31 173.0(3), C5–N5–C39 171.9(3), C6–N6–C47 170.8(4), av cis C–V–C 90(2), av trans C–V–C 177(2).

Table 3. Comparison of Structural and Infrared Data for $[V(CNXyl)_6]^z$

	Z = 1+	Z = 0	Z = 1–
av V–C (Å)	2.07(2)	2.026(7)	1.98(3)
av C–NXyl (Å)	1.169(6)	1.186(5)	1.20(2)
av C–N–C (deg)	173(2)	163(4)	158(10)
ν_{CN} in THF (cm^{-1})	2033	1939	1817
back-donation increases \rightarrow			

Table 3 summarizes structural and IR data for all three homoleptic vanadium isocyanides, **2**, **3**, and **4**. The trends presented in this table nicely parallel those obtained for the isoelectronic series $[Cr(CNPh)_6]^z$ ($z = 0, 1+, 2+$)^{57,63} and are consistent with the aryl isocyanides functioning as good π acceptor ligands. Among three structural parameters considered, the V–C bond length seems to be the most sensitive to changes in the vanadium oxidation state. Bending of the isocyanide ligands is the least reliable factor reflecting relative electron richness of the complexes. The latter is not surprising since, in addition to electronic effects, magnitudes of the C–N–C angles are greatly influenced by steric and interionic (e.g., as in **3**) interactions as well as crystal packing forces. Nevertheless, the C–N–C angles observed for **2** and **4** do correlate well with the corresponding V–C and C–NXyl distances and infrared ν_{CN} stretching frequencies of these species in the expected manner.

trans-V(CO)₂(CNXyl)₄ (5). Complex **5** crystallizes in the rarely encountered tetragonal space group $P4nc$. The structure of **5** is shown in Figure 5. It exhibits mutually trans V–CO units. The crystallographic 4-fold axis passes through the OC–V–CO fragment requiring molecular symmetry of **5** to be strictly C_4 . The xyllyl substituents of four equivalent isocyanide ligands feature a propeller-like arrangement with no unusually short Me \cdots Me contacts. Compound **5** is practically octahedral.

(63) Bohling, D. A.; Mann, K. R. *Inorg. Chem.* **1984**, *23*, 1426.

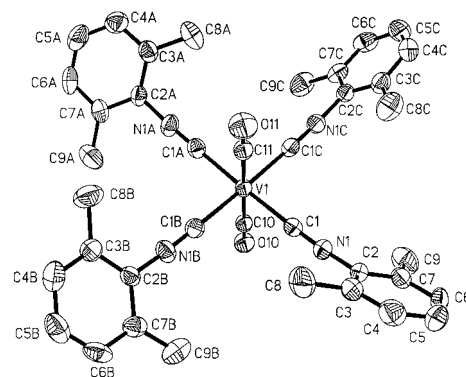


Figure 5. Molecular structure of **5** (50% thermal ellipsoids); hydrogens are omitted for clarity. Selected bond lengths (Å) and angles (deg): V–C1 2.044(2), V–C10 1.965(5), V–C11 1.944(6), C1–N1 1.170(2), C10–O10 1.154(6), C11–O11 1.150(7), C1–N1–C2 172.2(2), C10–V–C11 180.0, C1–V–C1A 176.2(2), C1–V–C1B 89.936(5), C1–V–C10 91.91(7), C1–V–C11 88.09(7).

Table 4. Comparison of V–CN and C–NXyl Distances (Å) and C–N–C Angles (deg) for **2**, **4**, **5**, and *trans*- $VI_2(CNXyl)_4$

	2	5	4	$VI_2(CNXyl)_4$ ^{10a}
av V–CN	2.026(7)	2.044(2)	2.07(2)	2.143(21)
av C–NXyl	1.186(5)	1.170(2)	1.169(6)	1.145(8)
av C–N–C	163(4)	172.2(2)	173(2)	176(4)

Table 5. Comparison of V–CO and C–O Distances (Å) for $V(CO)_6$,⁵⁶ **5**, and *trans*- $V(CO)_2(dmpe)_2$ ⁶⁴

	$V(CO)_6$	5	$V(CO)_2(dmpe)_2$
av V–CO	2.001(6)	1.955(15)	1.891(11)
av C–O	1.128(8)	1.152(7)	1.184(10)

As expected, the V–CO bonds are shorter than the V–CN distances within **5**. Judging by the V–CN bond lengths in **2**, **4**, **5**, and *trans*- $VI_2(CNXyl)_4$ ^{10a} (Table 4), the amount of electron density at the vanadium center, available for π bonding with CNXyl ligands, decreases in the row **2** > **5** > **4** > *trans*- $VI_2(CNXyl)_4$. The shortening of the V–CO bonds and the concomitant lengthening of the C–O distances in proceeding from $V(CO)_6$ ⁵⁶ through **5** to *trans*- $V(CO)_2(dmpe)_2$ ⁶⁴ (Table 5) nicely reflect the decrease in electron accepting capability in the series of ligands CO > CNXyl > dmpe.

Both steric and electronic factors favor the trans arrangement of the carbonyl ligands in **5**. While the steric argument is straightforward, the electronic reason is less obvious. The latter is based on the angular overlap considerations originally proposed by Bursten⁶⁵ and Mingos⁶⁶ for complexes $[ML'_2L_4]^z$, where L is a poorer π acceptor compared to L'. Figure 6 shows stabilization energies⁶⁷ of d_π orbitals for hypothetical *cis*- $V(CO)_2(CNXyl)_4$ and observed *trans*- $V(CO)_2(CNXyl)_4$, **5**, with respect to the t_{2g} -like set in **2**. It turns out that for the 17-electron complex $V(CO)_2(CNXyl)_4$, trans configuration leads to greater stabilization of five d electrons by means of back-donation to the CO ligands ($E_{stab}(trans) = 8\beta_\pi S_\pi^2$ vs $E_{stab}(cis) = 7\beta_\pi S_\pi^2$). On the other hand, a similar approach suggests that for an 18-

(64) Wells, F. J.; Wilkinson, G.; Motevalli, M.; Hursthouse, M. B. *Polyhedron* **1987**, *6*, 1351.

(65) Bursten, B. E. *J. Am. Chem. Soc.* **1982**, *104*, 1299.

(66) Mingos, D. M. P. *J. Organomet. Chem.* **1979**, *179*, C29.

(67) Stabilization energy, E_{stab} , is defined as $(\sum n_i) \times \beta_\pi S_\pi^2$, where N is the number of carbonyls interacting with a given d orbital, n is the number of electrons in that orbital, β_π is a constant, and S_π is the extent of overlap between the appropriate CO and metal π orbitals. See the following for details: Burdett, J. K. *Inorg. Chem.* **1975**, *14*, 375.

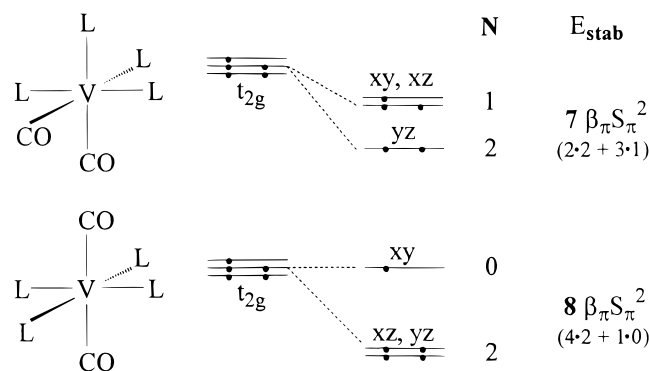


Figure 6. Stabilization energies (expressed as angular orbital functions)⁶⁷ of d_{π} orbitals for isomers $V(CO)_2L_4$ relative to the t_{2g} set of ML_6 ($L = CNXyl$). N is the number of carbonyls interacting with a given d orbital. (Based on diagrams from refs 65 and 66.)

electron low-spin d^6 species, such as $Mo(CO)_2(CNCy)_4$,⁶⁸ cis and trans isomers should be equally stable ($E_{stab}(cis) = E_{stab}(trans) = 8\beta_{\pi}S_{\pi}^2$). However, ligand–ligand overlaps, neglected in the angular overlap model,⁶⁶ make cis configuration more thermodynamically favorable in the case of $Mo(CO)_2(CNCy)_4$. The above arguments were previously used by Walton and Conner to explain why oxidation of *cis*- $Mo(CO)_2(CNCy)_4$ resulted in *trans*- $[Mo(CO)_2(CNCy)_4]^+$.⁶⁸ Exclusive formations of *trans*- $V(CO)_2(dmpe)_2$ ⁶⁴ (eq 3.28) and *cis*- $Cr(CO)_2(dmpe)_2$ ⁶⁹ were rationalized in a similar manner as well.

Magnetic Properties of 2–5: $V(CNXyl)_6$ (2). Complex **2** is the first paramagnetic homoleptic metal(0) isocyanide. Unlike $[M(CNXyl)_4]_2$ ($M = Co$,^{3b,5} Rh ⁷⁰), **2** is monomeric both in the solid state and in solution. Its effective magnetic moment of $1.76 \mu_B$ at 25 °C implies a low-spin d^5 configuration of **2** and is virtually identical with those reported for $V(CO)_6$ (1.73 – $1.78 \mu_B$)⁷¹ and $V(PF_3)_6$ ($1.76 \mu_B$).⁷² The diamagnetic correction, applied to molar susceptibility of **2**, was determined by measuring molar susceptibility of $Cr(CNXyl)_6$,²⁰ a low-spin d^6 complex. Such correction should be very accurate since the difference between diamagnetic susceptibilities of $V(0)$ and $Cr(0)$ is negligible.⁷³ The free ion spin–orbit coupling constant, λ , for $V(0)$ is about -95 cm^{-1} .⁷⁴ In the case of an octahedral low-spin d^5 species, $\lambda = -95 \text{ cm}^{-1}$ is expected to lead to a magnetic moment of ca. $2.3 \mu_B$ at 25 °C.⁷⁵ However, μ_{eff} of **2** as well as those of $V(CO)_6$, and $V(PF_3)_6$ are essentially “spin only”. Quenching of the orbital angular momentum in these compounds may be attributed, in part, to significant delocalization of unpaired electron density onto the ligands via back-donation.⁷⁶ Incidentally, μ_{eff} of $V(Me_2PCH_2CH_2PMe_2)_3$ (where the organophosphine ligand is a poor acceptor, at best) at 25 °C is $2.10 \mu_B$.⁷⁷ Also, the room-temperature effective magnetic moment increases within the isoelectronic series **2** ($1.76 \mu_B$) < $[Cr(CNXyl)_6][BF_4]$ ($1.92 \mu_B$) < and $[Mn(CNPh)_6][BF_4]_2$ ⁷⁸ ($2.32 \mu_B$). The latter compound exhibits only a very small degree of

Table 6. 1H and ^{13}C Paramagnetic Shifts of **2** and $7[BF_4]$ at 20 °C vs $Cr(CNXyl)_6$

nucleus	$\Delta\delta$, (ppm)	
	$V(CNXyl)_6^a$	$[Cr(CNXyl)_6]^+^b$
<i>o</i> -CH ₃	+7.04	+6.27
<i>m</i> -H	+7.18	+5.53
<i>p</i> -H	-9.20	-8.31
<i>i</i> -C	-225.7	-162.8
<i>o</i> -C	+205.8	+90.2
<i>o</i> -CH ₃	-23.6	-19.9
<i>m</i> -C	-25.8	-36.4
<i>p</i> -C	+54.1	+55.0

^a In $C_6D_5CD_3$. ^b In $CDCl_3$.

back-bonding and its μ_{eff} is practically identical with the value anticipated by the theory for a low-spin $Mn(2+)$ complex.⁷⁵

It is well-known that $V(CO)_6$ is ESR silent at ambient temperature.⁷⁹ No ESR signal could be detected for a toluene solution of **2** at 20 °C either. At the same time, relatively sharp 1H NMR resonances, showing strong paramagnetic shifts, were observed for **2** in C_6D_6 and $C_6D_5CD_3$. Both of these features are consistent with the very short electron spin relaxation time expected for a homoleptic octahedral low-spin d^5 complex $[ML_6]^z$.⁸⁰ The hydrogen NMR resonances for **2** were easily assigned based on their relative intensities and splitting due to H–H coupling and confirmed by an 1H COSY picture. Assignment of the ^{13}C NMR peaks for **2** was facilitated by an 1H – $^{13}C\{^1H\}$ HETCOR experiment. For the sake of comparison, $[Cr(CNXyl)_6][BF_4]$, **7** $[BF_4]$, was synthesized and its 1H , ^{13}C , and two-dimensional NMR spectra were recorded. To our great surprise, even though many homoleptic aryl isocyanides of $Cr(1+)$ have been known for a long time,²⁸ NMR data on such compounds have not been reported prior to this study.

1H and ^{13}C paramagnetic (isotropic) shifts of **2** and **7** $[BF_4]$, $\Delta\delta$, at 20 °C were determined relative to diamagnetic $Cr(CNXyl)_6$ (**6**) and are collated in Table 6. The NMR spectra of the reference compound **6** were obtained²⁷ in the appropriate media ($C_6D_5CD_3$ or $CDCl_3$) to minimize any solvent effects on the isotropic shifts of **2** and **7**.⁸¹ The hydrogen paramagnetic shifts of **2** and **7** are essentially contact in origin due to the approximately octahedral symmetry of these species.^{22,80} Indeed, as in the case of $V(CO)_6$,^{71b} the average g tensors for **2** and **7** are expected to be isotropic in solution (dynamic Jahn–Teller effect), so the dipolar field should be averaged to near zero by rapid tumbling of the complexes in solution. Also, since $\Delta\delta$ values, obtained for **7** $[BF_4]$, are practically insensitive to variations in solvent ($CDCl_3$ or $THF-d^8$) and concentration, any significant pseudocontact contributions to the 1H isotropic shifts of **7** due to ion pairing can be ruled out.⁸¹ As can be seen from Table 6, the 1H and ^{13}C isotropic shifts of **2** and **7** occur in both directions and do not attenuate with the increasing number of bonds from the metal center. This is consistent with unpaired spin being present in the π systems of the xylyl substituents. The *p*-C and *p*-H resonances are shifted in opposite directions (atomic exchange coupling mechanism of spin delocalization⁸²). The same applies to *m*-C and *m*-H signals. On the other hand, the carbon atoms in the ortho positions and the hydrogens of

(78) Nielson, R. M.; Wherland, S. *Inorg. Chem.* **1985**, *24*, 3458.

(79) (a) Pratt, D. W.; Myers, R. J. *J. Am. Chem. Soc.* **1967**, *89*, 6740.

(b) Rubinson, K. A. *J. Am. Chem. Soc.* **1976**, *98*, 5188. (c) Boyer, M. P.; Le Page, Y.; Morton, J. R.; Preston, K. F.; Vuolle, M. J. *Can. J. Spectrosc.* **1981**, *26*, 181.

(80) Drago, R. S. *Physical Methods in Chemistry*; W. B. Saunders: Philadelphia, PA, 1977; Chapter 12.

(81) Wicholas, M.; Drago, R. S. *J. Am. Chem. Soc.* **1969**, *91*, 5963.

(82) McConnell, H. M.; Chesnut, D. B. *J. Chem. Phys.*, **1958**, *28*, 107.

(68) Conner, K. A.; Walton, R. A. *Inorg. Chem.* **1986**, *25*, 4422.

(69) Salt, J. E.; Girolami, G. S.; Wilkinson, G.; Motevalli, M.; Thornton-Pett, M.; Hursthouse, M. B. *J. Chem. Soc., Dalton Trans.* **1985**, 685.

(70) Yamamoto, Y.; Yamazaki, H. *Bull. Chem. Soc. Jpn.* **1984**, *57*, 297.

(71) (a) Calderazzo, F.; Cini, R.; Corrandini, P.; Ercoli, R.; Natta, G. *Chem. Ind. (London)* **1960**, *79*, 500. (b) Bernier, J. C.; Kahn, O. *Chem. Phys. Lett.* **1973**, *19*, 414.

(72) Collong, W.; Kruck, T. *Chem. Ber.* **1990**, *123*, 1655.

(73) E. König, E. In *Zahlenwerte und Funktionen aus Naturwissenschaften und Technik*, 6th ed.; Landolt-Börnstein; Springer-Verlag: Berlin, 1966; Vol. 2, p 16.

(74) Dunn, T. M. *Trans. Faraday Soc.* **1961**, *57*, 1441.

(75) Figgis, B. N.; Lewis, J. *Progr. Inorg. Chem.* **1964**, *6*, 37.

(76) Gerloch, M.; Miller, J. R. *Progr. Inorg. Chem.* **1968**, *10*, 1.

(77) Chatt, J.; Watson, H. R. *J. Chem. Soc.* **1962**, 2545.

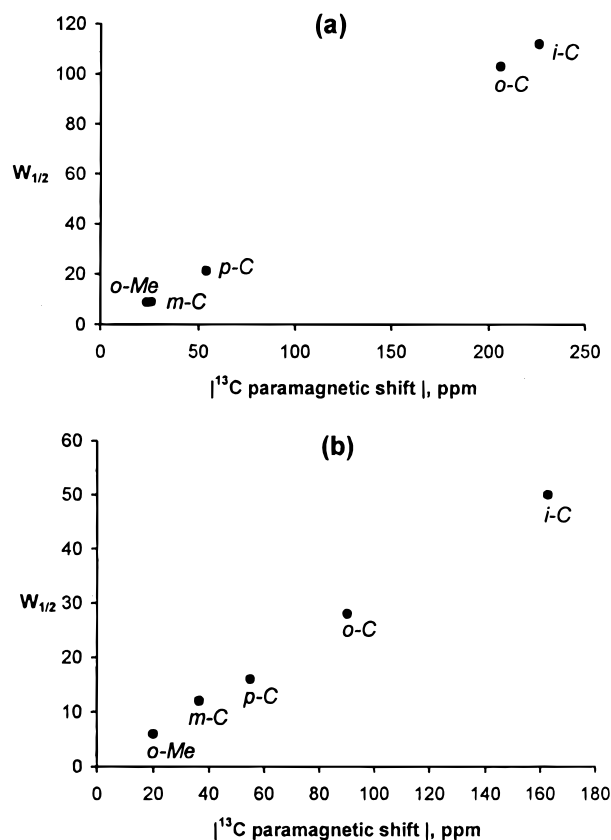


Figure 7. (a) Plot of ^{13}C line width vs magnitude of paramagnetic shift for **2** in $\text{C}_6\text{D}_5\text{CD}_3$ at 20°C . (b) Plot of the ^{13}C line width vs the magnitude of paramagnetic shift for **7**[BF_4] in CDCl_3 at 20°C .

the methyl groups exhibit paramagnetic shifts of the same sign, which is a consequence of hyperconjugative (direct) spin delocalization.⁸³ The directions of the ^{13}C paramagnetic shifts for **2** and **7** clearly indicate their predominantly contact nature and relatively minor importance of the so-called ligand-centered pseudocontact contribution.²² Interestingly, the line width at half-height ($W_{1/2}$) of the ^{13}C signals is nearly proportional to the magnitude of the paramagnetic shift. While the linearity of the relationships in Figure 7 has little physical significance, the general trends indicate the importance of contact relaxation for the carbon nuclei of **2** and **7**.⁸⁴ The slope in Figure 7a is greater than that in Figure 7b, which is consistent with more effective electron relaxation in the complex of higher charge.²²

The presence of unpaired spin in the π system of the aryl substituent of a coordinated ligand is not necessarily evidence for metal–ligand π -covalency.^{22,80,85} Nevertheless, since significant back-donation within compound **2** was unambiguously established by means of IR spectroscopy and X-ray crystallography (vide supra), $d\pi$ – $p\pi^*$ back-bonding may be expected to be an important contributor to the mechanism of unpaired spin delocalization in **2**. Signs of spin densities on the nuclei of the xylyl isocyanide ligands in **2** can be determined straightforwardly²² from the directions of the corresponding paramagnetic shifts (Figure 8). By definition, the spin on the metal center is aligned parallel to the field, i.e., it is positive or “ \uparrow ”.²² Even though the ^{13}C resonance of the terminal isocyanide

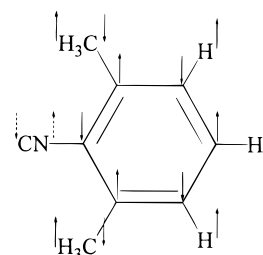
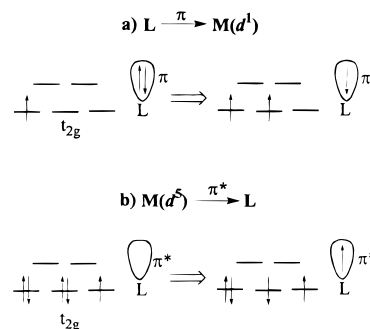


Figure 8. Signs of unpaired spin densities for the CNXyl ligands of **2** (\uparrow , positive; \downarrow , negative).

Scheme 2. Schematic Representation of Unpaired Electron Density Delocalization in a $d^1 \text{ML}_6$ Complex via $p\pi(\text{L})$ – $d\pi(\text{M})$ Bonding (a) and in a Low-Spin $d^5 \text{ML}_6$ Complex via $d\pi(\text{M})$ – $p\pi^*(\text{L})$ Back-Bonding (b) According to Ref 87



carbon was not experimentally observed for **2**, one can easily deduce⁸⁶ that this carbon must bear excess negative spin. Surprisingly, La Mar predicted the spin, induced on the ligating atom by means of π back-bonding, to be positive for a homoleptic octahedral low-spin d^5 complex.⁸⁷ To sort out this discrepancy, we considered ligand-to-metal $p\pi(\text{L})$ – $d\pi(\text{M})$ bonding in an octahedral d^1 complex and metal-to-ligand $d\pi(\text{M})$ – $p\pi^*(\text{L})$ back-bonding in a low-spin d^5 complex. Because of the electron–hole formalism, these two processes are topologically identical. According to La Mar,⁸⁷ ligand-to-metal π bonding in a d^1 octahedral complex should result in negative spin density on the ligand. Therefore, electron density will be transferred from filled π orbitals of L to t_{2g} orbitals of M slightly more with spin parallel to that on the metal (Scheme 2a). This should leave a net negative spin on the ligand. Such a delocalization mode is governed by correlation effects,⁸⁸ which, in simple terms, require maintaining the Hund’s rule at the metal center. Of course, the total spin of the complex remains unaffected by the $p\pi(\text{L})$ – $d\pi(\text{M})$ interaction. Now, if back-donation in the low-spin d^5 octahedral species produces excess positive spin on the ligand, delocalization of the electron density with excess spin parallel to that on the metal ion is implied (Scheme 2b). Such a process, however, violates the above-mentioned correlation requirements. On the other hand, if back-bonding in a low-spin d^5 octahedral complex involves transferring electrons possessing excess antiparallel spin, these requirements will be met. The latter mechanism is, in fact, consistent with the experimental results obtained for **2**.

Figure 9 shows Curie-type plots for ^1H paramagnetic shifts of **2** and **7**. In both cases, the contact shifts of the meta hydrogens follow the Curie law⁸² exactly within experimental

(83) Levy, D. H. *Mol. Phys.* **1966**, *10*, 233.

(84) (a) Bertini, I.; Luchinat, C. In *Physical Methods for Chemists*; Drago, R. S., Ed.; Saunders College Publishing: Philadelphia, PA, 1992. (b) Bloembergen, N. *J. Chem. Phys.*, **1957**, *27*, 575.

(85) (a) Fitzgerald, R. J.; Drago, R. S. *J. Am. Chem. Soc.* **1967**, *89*, 2879. (b) La Mar, G. N.; Sherman, E. O.; Fuchs, G. A. *J. Coord. Chem.* **1971**, *1*, 289.

(86) Horrocks, W. D., Jr.; Taylor, R. C.; La Mar, G. N. *J. Am. Chem. Soc.* **1964**, *86*, 3031.

(87) See ref 22, Table 3-VI on p 107.

(88) (a) Owen, J.; Thornley, J. H. M. *Rep. Prog. Phys.* **1966**, *29*, 675. (b) Orgel, L. *J. Chem. Phys.* **1959**, *30*, 1617. (c) Orgel, L. E. *Discuss. Faraday Soc.* **1958**, *26*, 92.

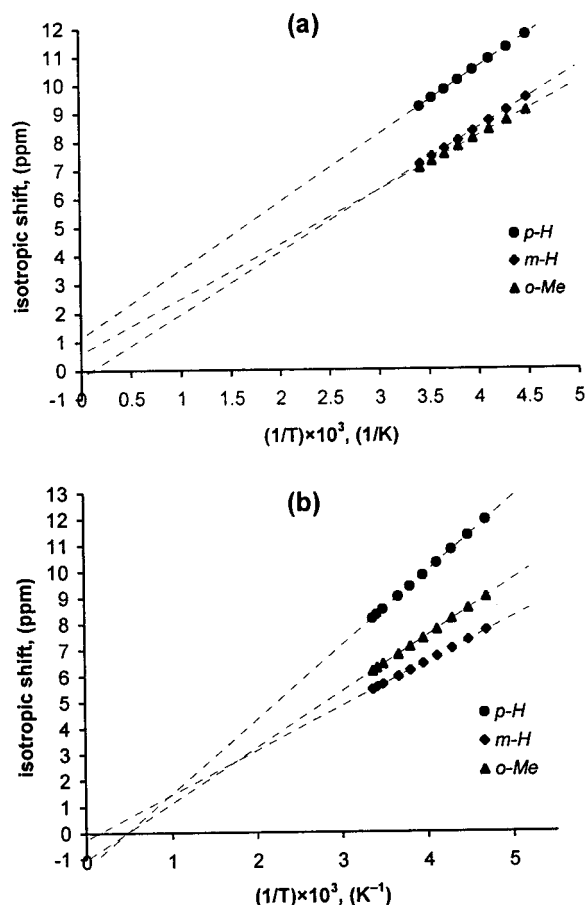


Figure 9. Curie plots for ^1H isotropic shifts of **2** (a) and **7**[BF_4] (b).

errors in the studied temperature ranges. On the other hand, intercepts obtained for the shifts of the para and methyl hydrogens are somewhat large to be attributed to experimental uncertainties. Complexes **2** and **7** possess degenerate T_{2g} ground states (assuming *ideal* octahedral symmetries), so their magnetic moments (and, hence, average g values) are not necessarily temperature independent.^{24a,80,84} This, in principle, may lead to deviations from the Curie law, which presupposes a constant isotropic g value.⁸⁹ Notably, however, the magnetic moments of both $\text{V}(\text{CO})_6$ ^{71b} and $\text{V}(\text{PF}_3)_6$ ⁷² are nearly constant in the temperature range considered for **2** and **7** in Figure 9. The use of equations,⁹⁰ derived for the contact isotropic shifts in an octahedral (t_{2g})⁵ field, could not explain the temperature behavior of the ^1H paramagnetic shifts observed for **2** and **7**. This fact is not surprising, in particular, because the free ion spin-orbit coupling constants, λ ,⁷⁴ employed in these equations are significantly altered by back-bonding, especially in the case of zerovalent **2**.

Taking into account the rather crowded nature of the CNXyl ligands (*vide infra*), it is reasonable to suggest that the above deviations from the Curie behavior may be caused, at least in part, by temperature dependence of the average orientation of the xylyl rings relative to the CN π systems.²² By analogy with the previous study on the benzyl radical,^{22,91} one might anticipate that at a given temperature the magnitude of the meta H contact shift will not change significantly upon rotation of the xylyl

(89) For recent discussions of theory of the paramagnetic shift for strong field d^5 complexes, see: McGarvey, B. R.; Batista, N. C.; Bezerra, C. W. B.; Schultz, M. S.; Franco, D. W. *Inorg. Chem.* **1998**, *37*, 2865 and references therein.

(90) Davis, D. G.; Kurland, R. J. *J. Chem. Phys.* **1967**, *46*, 388.

(91) Pople, J. A.; Beveridge, D. L. *J. Chem. Phys.* **1968**, *49*, 4725.

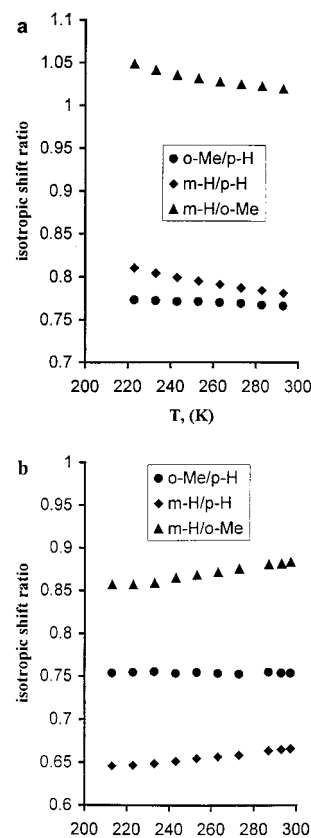


Figure 10. ^1H isotropic shift ratios for **1** (a) and **6** (b) vs temperature.

group around the N–Xyl bond and/or bending of the isocyanide ligand at nitrogen. This is a consequence of direct interaction of the aryl σ system with the π system of the CN group.⁹¹ At the same time, the ortho Me and para hydrogen shifts will be proportional to the overlap between the π systems of the CN and Xyl fragments. Should the analogy hold, for a $[\text{M}(\text{CNXyl})_6]^\pm$ complex the ratio $\Delta\delta(o\text{-Me})/\Delta\delta(p\text{-H})$ has to be nearly temperature independent while the ratios $\Delta\delta(m\text{-H})/\Delta\delta(p\text{-H})$ and $\Delta\delta(m\text{-H})/\Delta\delta(o\text{-Me})$ may vary with temperature. Figure 10 clearly illustrates that this, indeed, is the case for complexes **2** and **7**. Importantly, not only do the ratios $\Delta\delta(o\text{-Me})/\Delta\delta(p\text{-H})$ remain practically constant over the studied temperature intervals (circles in Figure 10), they are also of nearly the same magnitude for **2** and **7**. Thus, temperature dependence of the average orientation of the xylyl group with respect to the CN π system can reasonably account for the nonzero intercepts obtained for the para and methyl hydrogens in Figure 9. The paramagnetic shifts of the meta H resonances for **2** and **7** follow the Curie law rather accurately since, as in the case of benzyl radical,⁹¹ the magnitudes of meta H isotropic hyperfine coupling constants may not vary significantly with the orientation of the aryl substituents.

Finally, it is important to compare parameters $\Delta\delta^{\text{H}}/\mu_{\text{eff}}$ ⁹² for **2** and **7**. The ratios in eqs 1–3 are all greater than 1. This can be explained by greater contribution of $d\pi\text{--}p\pi^*$ back-bonding to the mechanism of unpaired spin delocalization for **2** than for **7**. The paramagnetic shifts of ortho methyl and para hydrogens reflect primarily the extent of unpaired spin delocalization into the π systems of the aromatic rings and, therefore, depend on the overlap between the relevant CN and Xyl π systems in **2** and **7**. This is why the magnitudes of the ratios in eqs 2 and 3

(92) To a first approximation, magnitude of a contact shift is proportional to the isotropic g -value and, therefore, to the magnetic moment of the complex.^{22,80,84}

are practically identical and remain the same over the studied temperature interval. Direct interaction of the meta hydrogens of the aryl substituents with unpaired spin in the CN π systems⁹¹ (vide infra) may account for the higher value of the ratio in eq 1.

$$\frac{\Delta\delta^{m-H}(2)}{\mu_{\text{eff}}(2)} / \frac{\Delta\delta^{m-H}(7)}{\mu_{\text{eff}}(7)} = 1.42 \quad (T = 293 \text{ K}) \quad (1)$$

$$\frac{\Delta\delta^{p-H}(2)}{\mu_{\text{eff}}(2)} / \frac{\Delta\delta^{p-H}(7)}{\mu_{\text{eff}}(7)} = 1.21 \quad (T = 293 \text{ K}) \quad (2)$$

$$\frac{\Delta\delta^{o-Me}(2)}{\mu_{\text{eff}}(2)} / \frac{\Delta\delta^{o-Me}(7)}{\mu_{\text{eff}}(7)} = 1.22 \quad (T = 293 \text{ K}) \quad (3)$$

[V(CNXyl)₆]⁻ (3). Pure Cs3 and [Cs(18-Crown-6)₂]**3** are diamagnetic in solution and in the solid state. They both exhibit ¹H and ¹³C NMR patterns consistent with equivalently bound 2,6-dimethylphenyl groups. These spectra closely resemble those obtained for the isoelectronic low-spin d⁶ Cr(CNXyl)₆²⁰ complex. As neutral **2**, anion **3** does not undergo rapid ligand exchange with free CNXyl. On the other hand, intermolecular electron transfer between **2** and **3** is very fast on the NMR time scale. Indeed, the room temperature ¹H and ¹³C NMR spectra of mixtures, containing **2** and **3**, constitute weighted averages of the patterns observed for the individual components.²⁷

[V(CNXyl)₆]⁺ (4). Complex **4**[PF₆]₂ is paramagnetic in the solid state with $\mu_{\text{eff}} = 2.74 \mu_{\text{B}}$ at room temperature, which is consistent with low-spin d⁴ configuration and octahedral geometry of **4**. Surprisingly, solutions of **4**[PF₆]₂ in THF were found to be only weakly paramagnetic as determined by the Evans method.²⁵ ¹H and ¹³C NMR spectra of **4**[PF₆]₂ in THF-*d*⁸ also indicated loss of the expected paramagnetism in solution.²⁷ Indeed, these spectra are almost identical with those of diamagnetic [M(CNXyl)₇]⁺ (M = Nb, Ta).^{9b} The ¹H NMR pattern of **4**[PF₆]₂ at room temperature consists of two somewhat broadened singlets at 2.25 (6H) and 7.13 ppm (3H) corresponding to methyl and aromatic hydrogens of the CNXyl ligands, respectively. Cooling the sample to -60 °C resulted in only very small (<0.1 ppm) downfield shifts of both resonances. Thus, the isocyanides in the complex are equivalent on the NMR time scale and did not undergo fast exchange with added free isocyanide. Room temperature ³¹P and ¹⁹F NMR spectra of **3**[PF₆]₂ were unexceptional and remained unchanged upon lowering the temperature to -100 °C. Moreover, substitution of the [PF₆]⁻ anion by either [BF₄]⁻ or [BPh₄]⁻ did not affect the ¹H NMR characteristics of the cation.²⁷ Changing the solvent from THF-*d*⁸ to CD₂Cl₂ resulted in practically the same ¹H and ¹³C NMR patterns for **4**[PF₆]₂. To check whether [Cr(CNXyl)₆]²⁺, isoelectronic with **4**, would exhibit similar behavior in solution, complex [Cr(CNXyl)₆][PF₆]₂ (**8**[PF₆]₂) was prepared. However, the ¹H NMR spectrum of this compound in CD₂Cl₂ was fully in accord with the anticipated ideal degenerate ³T_{1g} ground state of the octahedral low-spin d⁴ dication **8**.²⁷ As in the case of low-spin d⁵ **2** and **7**, strong ¹H paramagnetic shifts in both directions were observed for complex **7**. Their magnitudes increased with decreasing temperature and the *m-H* paramagnetic shift followed the Curie law exactly.

On the basis of the above facts, interaction of **4** with counterions can be safely ruled out as the cause of quenching of its paramagnetism in solution. Dimerization of **4**, either direct or through the aryl rings,⁹³ leading to antiferromagnetic coupling

of two vanadium(1+) centers seems to be unlikely because this does not happen with the isoelectronic low-spin d⁴ ion **8** and the related low-spin d⁵ complexes **2**, **7**, and [Mn(CNAr)₆]²⁺.⁷⁸ A reasonable hypothesis, which may account for the unusual magnetic behavior of **4**, would be severe distortion of the octahedral geometry of **4** in solution. In principle, the distortion may be caused by an interaction of **4** with the solvent. Such interaction, however, cannot be very strong since removal of the solvent (THF or CH₂Cl₂) from solutions of **4**[PF₆]₂ quantitatively regenerates the unsolvated and fully paramagnetic compound.

trans-V(CO)₂(CNXyl)₄ (5). Compound **5** possesses the effective magnetic moment of 1.75 μ_{B} at 22 °C in the solid state. This value is consistent with the low-spin d⁵ configuration of **5** and is virtually identical with $\mu_{\text{eff}} = 1.76$ and 1.73–1.78 μ_{B} obtained for **2** and V(CO)₆,⁷¹ respectively. The trans geometry of **5**, unambiguously established by X-ray crystallography (vide supra), implies a tetragonal distortion from octahedral symmetry.⁹⁴ The t_{2g}-like d orbitals of vanadium should be split into b (d_{xy}) and e (d_{xz}, d_{yz}) sets under C₄ symmetry. Since CO is a better π acceptor compared to CNXyl, the e orbitals must be lower in energy than the b orbital, leading to a nondegenerate ²B ground state of **5**. Therefore, one might anticipate the electron-spin relaxation time for **5** to be rather long.^{80,84a} In accord with this expectation, no ¹H NMR signals were detected for C₆D₆ solutions of **5** at room temperature. On the other hand, a reasonably resolved ESR spectrum of **5** was obtained in toluene glass. The latter appears to consist of two partially overlapping sets of eight equally spaced lines with $g_{\text{av}} = 2.023$ ($g_{\perp} = 2.038$, $g_{\parallel} = 1.993$). These *g* values are similar to those reported for the analogous low-spin d⁵ complexes *trans*-V(CO)₂(dmpe)₂⁶⁴ and *trans*-[Mo(CO)₂(CNCy)₄]⁺.⁹⁵ Hyperfine splitting ($A_{\perp} = 31$ G, $A_{\parallel} = 80$ G) in the ESR spectrum of **5** is due to interaction of the single electron spin with ⁵¹V nucleus ($I = 7/2$, 99.8%). The largest hyperfine coupling component corresponds to the smallest *g* component, which is consistent with a ²B ground state of **5** and, hence, trans geometry of this compound.⁹⁴ The average hyperfine splitting of 47 G, observed for **5**, is somewhat greater than $A_{\text{av}} = 36$ G, found for V(CO)₆ in toluene glass,^{79b} indicating that the vanadium center in the former species is more electron rich. This is, of course, due to CO being a better π acceptor compared to CNXyl. Of note, the average hyperfine coupling constants for bis(η^6 -naphthalene)-vanadium(0) and tris(2,2'-dipyridyl)vanadium(0) were reported to be 66¹⁸ and 83.5 G,⁹⁶ respectively.

Concluding Remarks

Syntheses of the first 16-, 17-, and 18-electron homoleptic isocyanides of vanadium, [V(CNXyl)₆]^z ($z = 1+$, 0, 1-), were successfully accomplished. These thermally stable but air-sensitive complexes were isolated in high yields and were carefully characterized by a variety of spectroscopic methods and X-ray crystallography. The bulky nature of xylyl isocyanide appears to be of critical importance for the stability of zerovalent V(CNXyl)₆, oxidation and reduction of which provided novel [V(CNXyl)₆]⁺ and [V(CNXyl)₆]⁻, respectively. Synthesis of *trans*-V(CO)₂(CNXyl)₄ under mild conditions is very remarkable in that no disproportionation of V(CO)₆ in the presence of xylyl isocyanide occurred. Both V(CNXyl)₆ and *trans*-V(CO)₂(CNXyl)₄ constitute the first examples of paramagnetic metal(0) compounds possessing at least one isocyanide ligand. The

(94) Rieger, P. H. *Coord. Chem. Rev.* **1994**, *135*, 203.

(95) Conner, K. A.; Walton, R. A. *Organometallics* **1983**, *2*, 169.

(96) König, E. *Z. Naturforsch.* **1964**, *19a*, 1139.

(93) Bond, A. M.; Colton, R. *Inorg. Chem.* **1976**, *15*, 2036.

average V–CN bond length in the described vanadium isocyanides is a sensitive function of the extent of back-bonding to the isocyanide ligands. This distance increases in the series $[\text{V}(\text{CNXyl})_6]^- < \text{V}(\text{CNXyl})_6 < \text{trans-V}(\text{CO})_2(\text{CNXyl})_4 < [\text{V}(\text{CNXyl})_6]^+$. The infrared cyanide ν_{CN} stretching frequencies also increase in the same order.

The vast majority of paramagnetic transition metal compounds, for which NMR spectra have been obtained, contain metals in positive oxidation states. Comparison of the NMR patterns for zerovalent **2** and monovalent **7** indicates the importance⁹⁷ of back-bonding in the mechanism of unpaired electron spin delocalization at least in the case of **2**. Contrary to the previous prediction for $d\pi(\text{M})-p\pi^*(\text{L})$ unpaired spin delocalization in low-spin d^5 octahedral complexes,⁸⁷ it appears that $d\pi(\text{V})-p\pi^*(\text{CNXyl})$ back-donation within **2** induces excess negative spin density (spin polarization) on the isocyanide ligands. This fact, however, is consistent with the correlation requirements at the vanadium(0) center.

Together with our other recent contribution,^{9b} this study clearly demonstrates the exceptional versatility of the 2,6-xylyl

(97) Strictly speaking, we can only conclude that back-bonding is an important but not necessarily dominant contributor²² to the mechanism of unpaired electron density delocalization within **2**. This caution is based on Drago's doubt^{85a} that unpaired electron density in the π systems of the aryl substituents of $[\text{Ni}(\text{NCPH})_6]^{2+}$ (Kluiber, R. W.; Horrocks, W. D., Jr. *Inorg. Chem.* **1966**, 5, 152) is a result of nickel–benzotrile π -bonding. Similarly, one has to be cautious invoking metal–ligand π -covalency to explain the NMR patterns obtained for $[\text{Mn}(\text{CNAr})_6]^{2+}$.⁷⁸

isocyanide ligand in stabilizing electron-rich group 5 transition metals. In particular, the existence of $[\text{V}(\text{CNXyl})_6]^-$, the first homoleptic octahedral isocyanide metalate,⁴¹ confirms the recent suggestion that the ability of isocyanides to form subvalent metal complexes has, indeed, been underestimated for decades.²⁸ The reaction chemistry of the electron rich vanadium isocyanides, reported herein, promises to be fruitful and is currently under examination. Also, extension of this research to group 4 transition elements is underway in this laboratory.

Acknowledgment. We dedicate this article to Professor M. L. H. Green on the occasion of his 65th birthday. The National Science Foundation and donors of the Petroleum Research Fund, administered by the American Chemical Society, are gratefully acknowledged for financial support. M.V.B. thanks the University of Minnesota for the 1998–1999 Doctoral Dissertation Fellowship. We are also indebted to Professor Kent R. Mann for valuable discussions.

Supporting Information Available: Details of crystallographic analyses for **2**, **Cs3**, **4**[PF₆], and **5**; complete tables of atomic coordinates, bond distances, angles, and anisotropic displacement parameters for the above structures (PDF). This material is available free of charge via the Internet at <http://pubs.acs.org>.

JA000212W